Sucrose-dependence of sugar uptake, quorum sensing and virulence of the rice blight pathogen *Xanthomonas oryzae* pv. *oryzae*

Mayuri Sadoine[1¶], Juying Long[2,3,¶], Congfeng Song[2,3,¶], Yugander Arra[1], Wolf B. Frommer[1,4,*] and Bing Yang[3,5,*]

[1] Institute for Molecular Physiology, Heinrich-Heine-University, Düsseldorf, Germany

[2] College of Plant Protection, Key Laboratory of Integrated Management of Crop Diseases and Pests, Ministry of Education, National Experimental Teaching Center for Plant Production, Nanjing Agricultural University, Nanjing 210095, China

[3] Department of Genetics, Development and Cell Biology, Iowa State University, Ames, IA 50011, USA

[4] Institute of Transformative Bio-Molecules (WPI-ITbM), Nagoya University, Nagoya, Japan

[5] Division of Plant Science and Technology, Bond Life Sciences Center, University of Missouri, Columbia, MO 65211, USA

[*] Corresponding authors: Bing Yang and Wolf B. Frommer

Email: yangbi@missouri.edu; frommew@hhu.de

[¶]These authors contributed equally to this work.

Abstract

Virulence of *Xanthomonas oryzae* pv. *oryzae* (*Xoo*), which causes bacterial blight of rice, depends on induction of host SWEET sucrose efflux transporters. It remained unknown whether secreted sucrose serves bacterial nutrition or host defense. Here we identified the *sux* sucrose uptake/utilization locus of *Xoo* and demonstrate that it is necessary and sufficient for sucrose acquisition. Induction of *sux* genes during infection closely tracked induction of rice *SWEET11a*. *sux* mutants were defective in swimming, swarming, extracellular polysaccharide (EPS) production and biofilm formation. EPS synthesis in mutants was restored by the quorum-sensing factor DSF. Notably, transcripts for rate limiting steps in DSF production were unaffected by sucrose, transcripts of the DSF receptor were sucrose-inducible and increased during infection, indicating sensitization to DSF in response to sucrose supply. Sucrose induced the sigma factors RpoN1 and RpoN2 that regulate swimming, EPS and virulence. Furthermore, in contrast to *Xanthomonas axonopodis* pv. *manihotis*, virulence of *Xoo* depended critically on *sux* gene function. Together, pathogen-induced sucrose efflux from host cells likely induces bacterial sigma factors and sensitizes quorum signaling necessary for biofilm formation and colonization of the xylem, serves as energy source for swimming against the xylem stream, and as nutrient for growth.

Author summary

If we want to efficiently protect plants against infections, we need to understand the disease mechanisms. Bacterial blight is a major scourge for rice production in Asia and Africa. We had found that disease-causing bacteria use a set of keys, so-called TAL effectors, to switch on sugar transporter genes in rice leaves causing sucrose release around the bacteria. A key question was whether the sugars act primarily in activation of host defense, or serve as nutrients and signals for bacterial infection. Here we provide evidence that both the ability to attack as well as the growth of bacteria depend on sucrose uptake. We unravel a regulatory network including transcriptional regulators, quorum sensing, swimming, biofilm production and virulence that all depend on sucrose uptake. These discoveries may prove to be crucial for the development of strategies for protecting rice against this disease.

Introduction

Diseases massively decrease global rice production (1). Bacterial blight (BB) is among the most damaging diseases in rice. Yield loss due to the causative bacterium *Xanthomonas oryzae* pv. *oryzae* (*Xoo*) is estimated to be up to 50 %, mostly in tropical and sub-tropical areas (2). *Xoo* is a vascular pathogen that enters rice leaves through water pores and wounds and subsequently colonizes the water-conducting xylem vessels (3). Colonization of the xylem, a unique niche, presents a major challenge to *Xoo*. Vascular wilt pathogens may exploit this niche to avoid competition with other microbes (4). However, the bacteria must colonize the xylem against the high flow rates of the xylem sap (5,6), which is generally faster than the bacterial swimming velocity (7). Moreover, the oxygen tension in the xylem is low, so incomplete oxidation requires higher amounts of carbohydrates from the pathogen (8). A further challenge is the comparatively low sugar concentration in the xylem sap (9–13). If we assume that guttation fluid could be a proxy for xylem sap composition, sugar levels are likely insufficient, since freeze-dried guttation fluid does not support growth of *Xoo* (14). This potential shortage of sugar components may limit *in planta* growth of *Xoo*. Since glucokinase gene (*glk*) mRNA levels increase under low oxygen tension and since *glk* mutants show impaired pathogenicity, it has been hypothesized that carbon and energy could possibly derive from uptake of glucose by the pathogen (15). However, the microbial phosphoenolpyruvate-dependent phosphotransferase system (PTS) for glucose uptake, which is essential for glucose uptake by *Xoo in vitro*, was not required for virulence (16).

Bacteria that manage to migrate against the xylem stream need to find a suitable hold where they can attach to living cells in the xylem in order to engage the type-III secretion system (T3SS) that enables injection of effector molecules into the living host cells, here the xylem parenchyma (17–22). The details for this remain unknown for *Xoo*, but *Erwinia amylovora* attaches to the xylem wall with the help of fimbriae (23). Much like the near-surface swimming of *Salmonella* in animal and human intestines, it is conceivable that *Xoo* also switches to a swimming mode before using fimbriae or T3SS components to attach to prominent surface features protected from the main xylem flow (24,25).

Virulence of *Xoo* is triggered by quorum-sensing (QS) factors that are secreted by the bacteria (26). *Xoo* also uses QS molecules that are distinct from those studied predominantly in the animal systems, and include the diffusible signal factor AHLs, DSF (*cis*-11-methyl-2-dodecenoic acid) and BDSF (*cis*-2-dodecenoic acid), which are intermediate chain fatty acids. In *Xoo*, DSF and BDSF are key signaling molecules involved in the control of virulence in response to cell density (27–29). Living in the xylem creates another unique challenge for the bacteria, since sap flow dilutes the secreted QS factors. Biofilm may protect quorum sensing factors from wash out. In *Pseudomonas aeruginosa*, either increased production of the QS factor acyl-homoserine lactone (HSL), or increased sensitivity to HSL, may contribute to effective quorum sensing in conditions of surrounding fluid flow (30) (31). Polymers secreted by pathogens, such as EPS play a role in various aspects of the infection process, namely bacterial adhesion on host cell surfaces, cohesion

of colonies and providing a protected domain. During colonization, *Xoo* secretes exopolysaccharides (EPS; here xanthan gum) and uses swarming to produce biofilm. EPS production, swarming motility and biofilm formation under control of quorum sensing (26). While in some cases swarming motility and EPS production have been shown to play roles in virulence, several *Xoo* mutants with reduced EPS production did not show altered virulence in rice (32). EPS is a virulence factor in many bacterial species, (33–36). In *Xoo,* EPS levels and virulence were found to be correlated when comparing >100 different isolates (37). Moreover, analysis of a wide range of *Xoo* mutants supports a tight link between EPS content and virulence as well. Notably, a mutant in the acetyltransferase gene *gumG* was impaired with respect to EPS production and virulence (38). Taken together, both colonization and bacterial proliferation in the xylem likely requires substantial amounts of carbon and energy in early infection process.

After establishment of the T3SS, *Xoo* injects a variety of effector proteins, including members of a family of diverse TAL effectors (TALe, transcriptional activator-like effectors), as key virulence factors (39). TALes transcriptionally activate various host genes, in particular genes encoding sucrose transporters in the SWEET family (17,40–42). In this way, bacteria divert the sucrose flux of the host into the xylem apoplasm (22,43–45). This indicates that acquisition of sucrose from the host is important for *Xoo* proliferation *in planta*. When leaf clipping introduces bacteria into the wounded surface, local bacterial growth is largely independent of SWEETs, while the spread is fully SWEET-dependent (46). This indicates that SWEETs are important, particularly for migration and colonization of the xylem by *Xoo*. Notably, all known pathogenic *Xoo* strains depend on induction of SWEET genes, a feature that has been exploited to generate broad-spectrum resistance against bacterial blight by blocking the ability of *Xoo* to induce SWEET sucrose transporters (47,48). Remaining questions include whether the host-derived sucrose serves to support colonization of the xylem and rapid reproduction or as a signal for the host that induces defense responses (49).

Glucose-transporting SWEETs are not able to support *Xoo* infection and a glucose uptake-deficient *Xoo* mutant was able to colonize and proliferate in the xylem, therefore sucrose released from the host's xylem cells via SWEETs may provide the prime carbon and energy in places accessible to the bacteria (16,50). We therefore searched for potential sucrose acquisition components in *Xoo*. Genomes of Gram-negative, phytopathogenic bacteria, and Xanthomonads in particular, show an enrichment of transport systems that make use of TonB-dependent receptors (TBDR) (51). A substantial number of these are part of so-called CUT (carbohydrate utilization) loci. Among them are 'sucrose utilization loci' that are composed of genes encoding TBDR outer membrane transporters, inner membrane transporters, hydrolytic enzymes, and SuxR transcriptional regulators. Analysis of the virulence of 76 TBDR mutants led to the identification of the gene XCC3358 from *Xanthomonas campestris* pv. *campestris* (*Xcc*), mutants of which showed delayed symptom development in Arabidopsis. Mutations in the sucrose hydrolase gene, a component of a related locus from *Xanthomonas axonopodis* pv. *glycines (Xag)*, showed moderately delayed symptom development (52). In contrast, mutation of the *suxC* gene, corresponding to the inner membrane

transporter, did not affect the virulence of *Xanthomonas axonopodis* pv. *manihotis (Xam)* (53). Thus, the relevance of sucrose uptake for virulence may differ between *Xanthomonas* species and remains unknown for *Xoo*. To gain insight into sucrose utilization and any correlation between sucrose metabolism and pathogenicity, we characterized four genes in the *sux* locus in *Xoo* and found that it is necessary and sufficient for sucrose uptake, for efficient growth on sucrose, for swimming, swarming, EPS production, and biofilm formation, and, importantly, for virulence. Sucrose triggered transcriptional regulation and supplementation of EPS deficiency by the quorum-sensing factor DSF indicate that, besides roles in carbon and energy supply, sucrose or its downstream products also serve as signals to promotes vital bacterial functions during colonization.

Results

Identification of a cluster of sucrose utilization genes in Xoo

To determine if *Xoo* is capable of acquiring host-derived sucrose and to identify sucrose uptake systems in the pathogen, we searched for potential sucrose utilization loci in the genome of *Xoo* strain PXO99^{A}. Sucrose utilization loci have been identified in several phytopathogenic *Xanthomonas* species (51). Homology searches using *suxA* from *Xcc* (XCC3358, encoding a TBDR functioning as an outer membrane sucrose transporter) (51), identified an 87 % identical gene, PXO_02415, which was thus named *suxA* (Table 1, S1 Fig and S1 Table). Additional components (PXO_02412, PXO_02413 and PXO_02416) were found in the same locus with 87 %, 88 % and 81 % identity to *suxR*, *suxC*, and *suxB* of *Xcc*, respectively (Table 1; S1 Fig and S1 Table). While *suxR* and *suxC* are mono-cistronic, each with their own predicted promoters, namely pR and pC, *suxA* and *suxB* are polycistronic and are possibly controlled by the single promoter pAB (S1 Fig). The components and spatial arrangement of the *sux* gene cluster are highly conserved among *Xanthomonas* spp. (S2 Fig, S2 Table).

Table 1. Components of the *sux* locus of *Xoo*

Locus id PXO99^{A}	Protein id PXO99^{A}	Gene name	Protein name	Putative function
PXO_02412	ACD60701.1	*suxR*	SuxR	LacI type HDH* domain transcriptional regulator
PXO_02413	ACD60702.1	*suxC*	SuxC	Inner membrane MFS**-type sugar transporter
PXO_02415	ACD60703.1	*suxA*	SuxA	TonB***-dependent receptor, β-barrel outer membrane transporter
PXO_02416	ACD60704.1	*suxB*	SuxB	amylosucrase, sucrose hydrolase

* Helix-Turn-Helix
** Major Facilitator Superfamily
*** Glycoside Hydrolase Family 13 (www.cazy.org)

Sucrose-specific derepression of sux genes

To test whether *sux* genes are upregulated during infection or are subject to regulation by sucrose, mRNA levels of *suxA*, *suxB* and *suxC* were quantified by qRT-PCR *in planta* and *in vitro* (Fig 1 and S3 Fig). Concomitant increases in *SWEET11a* and *sux* transcripts were detected in infected rice leaves 3 days post infection (dpi), and increased further over time, consistent with progressive infection of the host by *Xoo* (Fig 1a and S3b Fig). Since *Xoo* triggers TALe-mediated sucrose release by SWEETs from host cells, it is conceivable that SWEET-derived sucrose could serve as a signal for *sux* gene derepression/induction. Indeed, the parallel increase of transcript levels of *SWEET11a* and *suxB* is consistent with the induction of the *sux* gene cluster by host-derived sucrose (Fig 1b). Analysis of *suxB* and *suxC* mRNA levels in *Xoo* cultured in the presence and absence of sucrose showed that *suxB* and *suxC* mRNA levels increased ~25- and ~18-fold, respectively, in the presence of 1 % sucrose (29 mM; Fig 1c). The induction was sucrose-specific, since transcript levels for *suxB* and *suxC* were not substantially elevated in the presence of glucose (Fig 1c).

SuxR is a member of the *lac* repressor family and may thus function as a sucrose-dependent repressor of the *sux* gene promoters pAB and pC. The transcriptional regulator SuxR displays two conserved functional domains from the LacI family of bacterial regulatory proteins (Pfam IDs: PF13377.6, PF00532.21, PF00356.21, PF13407.6). An alignment of the promoter regions of *suxA/B* and *suxC* with the predicted binding motif of SuxR homologs from *Xam* and *Xag* from RegPrecise database identified a putative binding site for SuxR in *Xoo* (54). A homology model of SuxR based on its homolog CelR (PDB ID: 5ysz) indicates the presence of an N-terminal helix-turn-helix DNA binding domain and a C-terminal ligand binding domain. The sugar binding domain undergoes conformational rearrangement upon sugar binding which allosterically alters the affinity of the regulator to the DNA binding site (S3 Fig).

To determine whether SuxR might be involved in repression of *suxC* and *suxB*, mRNA levels were quantified in the Δ*suxR* strain. The mRNA of *suxB* and *suxC* were ~25 and ~58 times higher, respectively, in the Δ*suxR* mutants relative to wild type PXO99^{A}, when grown on full synthetic NB medium without addition of sugar (Fig 1c). Addition of glucose or sucrose had no effect in the Δ*suxR* mutant (S3c Fig) These results show that SuxR of *Xoo* strain PXO99^{A} is a negative regulator of the *sux* gene cluster in response to the disaccharide sucrose but not for the monosaccharide glucose. These data indicate that sucrose serves as a signal. It might be interesting to analyze whether SuxR function is restricted to the two *sux* promoters or whether it is involved in regulation of other targets that play roles in virulence.

Sux gene function is necessary for sucrose uptake

To determine if the sucrose utilization locus of *Xoo* is involved in bacterial multiplication, we examined the role of the *sux* gene cluster by monitoring bacterial growth on different media (Fig 2 and S4 Fig). On rich media (NBN) containing 1 %

sucrose, growth of PXO99^A was sucrose-dependent (Fig 2c and S4a, b Fig). Growth of *Δsux* on NBN with 1 % sucrose was impaired, but grew similar to PXO99^A on NBN with 1 % of glucose. Δ*sux* colony diameters were substantially smaller compared to PXO99^A on solid NBN containing 1 % sucrose (S4a, b Fig). *Xoo* does not grow on minimal mineral media but requires a variety of supplements such as amino acids and sugars (55). On minimal medium supplemented with glutamate, methionine and sucrose (NSM), growth of the *Δsux* mutant was severely compromised and never reached the same Optical Density (OD_{600}) as the control, PXO99^A (Fig 2d), while replacement of sucrose by glucose fully restored growth of mutant to the wild type level, demonstrating that the *sux* gene cluster provides the dominant sucrose uptake system in *Xoo*. Thus, both on basal and rich media, the *sux* genes are necessary for growth in the presence of sucrose. Glucose also supported growth of PXO99^A, and, as expected for a gene cluster involved in sucrose uptake, growth on glucose containing media (55 mM) was only slightly reduced on solid media relative to growth on sucrose (S4a, b Fig). Amylosucrase was essential, since Δ*suxB* showed a growth defect as severe as that of the Δ*sux* mutant, in which all *sux* genes were deleted. Complementation with the *suxB* gene restored growth on sucrose to wild-type levels (S4b Fig). Similarly, the inner membrane MFS transporter SuxC was essential, while mutation of the TBDR SuxA or the LacI-type repressor SuxR had a weaker or no effect (S4a, b Fig). The lower efficacy may be due to the redundancy of TBDRs (51), and the role of SuxR as a negative regulator. SuxC deficiency could be rescued by complementation (S4a, b Fig). While these data demonstrate the importance of the *sux* gene cluster and its major role in sucrose uptake and utilization, the media used for the growth assays contained other nutrients that can also serve as carbon sources. It was therefore not possible to exclude that other sucrose uptake mechanisms provide some residual activity. To directly determine if the inner membrane MFS transporter SuxC is responsible for sucrose uptake, PXO99^A and the Δ*suxC* mutant were transformed with the genetically encoded FRET sensor FLIPsuc-90μΔ1V (ref. (56)), and cytosolic sucrose accumulation was analyzed by monitoring the eYFP/eCFP emission ratio (Fig 2e). The saturating negative ratio change in response to sucrose addition was consistent with sucrose uptake in PXO99^A and binding of sucrose leading to a decrease in the eYFP/eCFP emission ratio (Fig 2e). The sensor did not report sucrose accumulation in the mutant (Fig 2e). Taken together, the data provide strong evidence that the *sux* gene cluster is necessary for uptake and utilization of sucrose as both a carbon and an energy source required for efficient reproduction.

Sux gene function is necessary for swimming and swarming motility

Colonization of the xylem after entry via hydathodes requires motility. Two mutants, Δ*sux* and a representative Δ*suxB* mutants, were tested for swimming motility on semi-solid media with 0.3 % agar. Both mutants showed a significant reduction in apparent swimming motility, indicating that sucrose may not only be required for efficient reproduction, but also motility (Fig 3a and S5a). Efficient colonization of the xylem requires progressive infection against the xylem stream, an activity requiring high amounts of energy, especially in a low-oxygen environment such as the xylem. Swarming is required for the generation of biofilm,

which is likely important for colonization of xylem vessel walls during infection. Similar to swimming, swarming also requires energy. Assays performed on semi-solid media with 0.6 % agar showed that the apparent swarming motility of Δ*sux* and Δ*suxB* mutants was impaired (Fig 3b). Of note, cell growth of the mutants was impaired, thus some of the reduction in apparent motility may be due to lower cell numbers. Twitching assays with Δ*sux* mutants showed that twitching motility was impaired as well (S5c Fig). In many bacterial species EPS increases 'wetness', thereby providing conditions for the flagella to function in swarming (57). In addition to requiring energy, swarming motility could also be limited due to a reduction in EPS production in the *sux* mutants. Derepression of the gene cluster in Δ*suxR* did not show detectable differences in swimming or swarming motility (S6 Fig).

Sucrose is necessary for EPS production and biofilm formation

EPS and biofilm production require both carbon and energy sources. Deficiency in EPS production causes changes in colony phenotype. For instance, PXO99^{A} colonies are smooth, mucoid, and shiny, while EPS mutants lose these features and become drier and flatter. On sucrose-containing media, colonies of Δ*sux,* Δ*suxC*, and Δ*suxB* mutants had EPS-deficiency phenotypes, while EPS production of Δ*suxA* and Δ*suxR* mutants did not seem to be affected, probably due to the existence of redundant TBDR functions (51) (S4 and S7a, c Fig). Consistent with a role of suxR as a repressor of the pAB and pC promoters, Δ*suxR* mutants produced wild-type-like colonies and did not display EPS-deficiency phenotypes (S4 Fig and S7b Fig). The Δ*suxC* mutant had a less severe colony phenotype, possibly indicating that sucrose may be processed partially outside the cytosol (*e.g.,* in the periplasmic space of the bacteria or the interface between host and bacteria;S4 Fig). The EPS-deficiency was rescued by complementation of the mutated *sux* genes (S4 Fig). PXO99^{A} produced about 30 mg of dry EPS per 10 mL culture when grown in liquid medium containing 1 % sucrose, while Δ*suxB* and Δ*sux* mutants produced ~20- and ~30-fold less EPS, respectively (Fig 4a, b and S8 Fig). When sugar was omitted, both wild-type and mutant colonies were small and EPS levels were lower than levels in presence of sucrose (Fig 4a, b and S4 and S8 Fig). Complementation of the mutants restored EPS production (S4 Fig and S9 Fig). Addition of glucose rescued EPS production in the mutants almost to wild-type levels (Fig 4a, S4 and S8 Fig). Since swarming is a prerequisite for proper biofilm formation and EPS is a key component of biofilm, biofilm formation was assessed. In the Δ*sux* and Δ*suxB* mutants, biofilm formation was reduced by about 75 % (Fig 4c and S10 Fig). Notably, EPS levels were reduced 10-fold, and biofilm production had showed a drastic sucrose-dependent reduction of about 75 %. Taken together, the data show that sucrose uptake is necessary for EPS production and biofilm formation.

Effects of sucrose supply on quorum sensing

In several *Xanthomonas* species, swimming, swarming, EPS production and biofilm formation are triggered by quorum-sensing factors (58). In *Xoo*, quorum sensing has been shown to affect bacterial swarming motility (59). We hypothesized that *sux* mutants might be impaired in quorum sensing, which would affect their ability to produce EPS. To test the hypothesis, EPS production was

measured in the presence or absence of externally supplied *Xoo* quorum-sensing factor DSF (Fig 4b). Notably, EPS production was sugar dependent, and DSF was able to partially restore EPS production in Δ*sux* and Δ*suxB* mutants (Fig 4b). DSF had no effect in the absence of sugars (Fig 4b). Glucose was able to restore EPS production, but not to the same levels as sucrose (Fig 4b). Similarly, external supply of DSF partially restored biofilm formation; consistent with the role of swarming for biofilm production (Fig 4d). The dependency of many of the observed *sux* phenotypes on quorum sensing and the observation that DSF can supplement EPS production in *sux* mutants and may indicate that sucrose plays a role in triggering quorum sensing. To test the effect of the infection on the key quorum sensing genes, The accumulation of *SWEET11a* mRNA and transcripts of the rate limiting enzyme RpfF, the DSF receptor histidine kinase (HK), RpfC, and the dual function response regulator and cyclic di-GMP phosphodiesterase, RpfG, were quantified in infected leaves (Fig 5a). Within 5 days post infection, *SWEET11a* and the *suxB* transcripts accumulated to high levels, and while *rpfF* transcripts were only marginally increased, *rpfC* and *rpfG* levels were also ~200-fold higher in the bacteria, indicating that *Xoo* increases the amount of receptor and signaling components to sensitize the responsiveness of *Xoo* cells to DSF. Host-derived sucrose appears to cause the sensitization, since sucrose is able to also trigger elevation of *rpfC* and *rpfG* transcripts *in vitro* after 2, 4 and 6 hours of cultivation, a time window in which the *sux* genes are induced (Fig 5b, e and S11 Fig). Glucose had a similar effect, but was 4-5-fold less efficient at the same molar concentration. Sigma (σ) factors serve as bacterial master regulators, and the σ^{54} factor RpoN2 from *Xanthomonas* ssp. is essential for motility, EPS production and virulence (60). The suite of phenotypes observed for *sux* mutants here is consistent with a contribution of sucrose-dependent regulation of σ^{54} transcript levels, which in turn plays important roles in colonization and virulence, although likely other factors in the complex c-di-GMP network also play important roles. This hypothesis would predict that *RpoN1* and *RpoN2* from *Xoo* are inducible by sucrose. Consistent with this model, *RpoN1* and *RpoN2* transcripts increased 5- to 6-fold when sucrose was added, while glucose had a much weaker effect (Fig 5c, e). *Gum* genes are responsible for EPS production and are under control of RpoN1 and RpoN2 (60). Consistent with the model, *gum* genes were found to be inducible by sucrose and to a lesser extent by glucose (Fig 5d, e). Notably, *SuxR* derepression in a Δ*suxR* mutant led to a 3- to 6-fold increase in *RpoN1* and *RpoN2* and *gum* transcript levels compared to the wild-type (Fig 5c,d, e and S12 Fig), intimating that SuxR might partially be responsible of the sucrose-dependent regulation of *RpoN1, RpoN2 and gum genes*. Derepression of *SuxR* did not lead to a measurable increase of *rpfF* and *rpfC* transcript levels and to only 2-fold increase in *rpfG* transcripts (Fig. 5b, e and S12 Fig).

Together these findings indicate that sucrose, or downstream products, serve as signals or allosteric regulators that act, at least in part, via σ^{54} to trigger a wide range of processes required for xylem colonization and virulence, in particular

sensitization to quorum sensing factors, flagellar assembly, and EPS production (60) (Fig 7).

sux genes are required for full pathogenicity

For some bacteria, swimming, swarming, EPS production and biofilm formation are necessary for virulence (58,61). For instance, *suxB* mutation has moderate effects on virulence of *Xag* in soybean, and *sux* mutations delay symptom development in Arabidopsis infected with *Xcc* (52). On the other hand, the *sux* genes are not required for virulence of *Xam* in cassava (53). The diverse phenotypes in key functions in the *Xoo* mutants described above make it likely that *Xoo* virulence is severely impaired in the *sux* mutants. Clipping assays using *Xoo* mutants were performed on *Oryza sativa* ssp. *japonica cv.* Kitaake. Δ*sux* mutants showed substantial decreases in virulence (Fig 6a, b). Therefore, for rice blight, the *sux* gene cluster functions as a key virulence factor. The remaining virulence could be due to a parallel pathway that enables sucrose hydrolysis, *e.g.*, invertases secreted by the host and subsequent acquisition via hexose transporters.

To determine the contribution of each *sux* genes to virulence, the individual *sux* mutants were tested as well. Likely due to the redundancy described above for TBDRs, Δ*suxA* impaired virulence only slightly. The Δ*suxR* mutant did not show a substantial reduction in virulence, which was also expected since SuxR functions as a negative regulatory factor (Fig 6a, b). In contrast, the Δ*suxC* and Δ*suxB* mutants showed a similar reduction in virulence as Δ*sux* (Fig 6a, b). Complementation with respective genes under control of the *E. coli* lac promoter almost completely restored virulence of the mutants (S13 Fig). Complementation of the mutants using constructs expressing the genes under their own promoters yielded similar levels of virulence restoration (S13 Fig). In summary, the *sux* gene cluster encodes an important function necessary for full virulence, and connects *Xoo*-induced expression of the host SWEET transporters to carbon and energy supplies as well as signaling processes required for motility and adhesion (Fig 7).

Discussion

Pathogens infect plants in order to gain access to host nutrients needed for effective reproduction. The ability of *Xoo* to directly induce *SWEET* sucrose transporter genes in the host xylem parenchyma led to the hypothesis that SWEETs release sucrose that serves as carbon and energy for *Xoo*. The key questions pursued here are whether *Xoo* can acquire sucrose, what the mechanisms for uptake and utilization are, how the processes are regulated in *Xoo* and whether the sucrose utilization systems are necessary for virulence. Here we identified the *sux* locus as a candidate for sucrose utilization in PXO99^{A} and showed that it is necessary for sucrose uptake and for growth of *Xoo* on sucrose. Since swimming motility is also severely impaired in the mutants, sucrose likely is required for migration in the xylem as well. The motility provided by the flagella is insufficient for swimming against the xylem stream, but may be useful either for swimming in the vicinity of the surface where different streaming conditions (Marangoni effect) prevail or during periods of xylem cavitation that frequently

occur (62). Loss of sucrose uptake activity had additional negative effects, such as drastically reduced EPS production. Since EPS is polysaccharide, host-derived sucrose likely serves as a source of carbon, and possibly energy, for its biosynthesis. Surprisingly, EPS production could be complemented by the quorum-sensing factor DSF, indicating that sucrose might also serves as a signal, here to induce DSF production, although this was not demonstrated directly. Since EPS is a major component of biofilm, and since swarming motility, necessary for biofilm formation, was also impaired in the mutants, it was not surprising that biofilm formation was also reduced in *sux* mutants. These multiple effects led to substantial impairment of virulence in the mutants impaired in sucrose uptake and utilization. Not all genes in the cluster contributed equally. SuxB (amylosucrase) and SuxC (inner membrane MFS superfamily transporter) were dominant players, while defects in SuxA, (outer membrane TBDR) had less severe effects, probably due to redundancy (51).

As one may expect, derepression of the sux genes in Δ*suxR* mutants neither affected EPS production nor swarming or swimming motility or biofilm production. Consistent with these observations, Δ*suxR* mutants did not show discernible effects on virulence, likely because it is not required for sucrose uptake *in planta.* It is however conceivable that the Δ*suxR* mutant may be less competitive due to the cost of constitutive activity of the cluster.

With the new data, we hypothesize the following path of infection: after entry into hydathodes and subsequent propagation in the epitheme, the bacterial cells swim upstream against the flow within the xylem and find suitable niches for attachment and injection of TALes like PthXo1. The TALes trigger release of sucrose, which is used both as a carbon source and an energy source as well as a signal triggering biofilm production. At present, the exact order of events remains unclear, since the xylem stream will likely dilute the quorum signal very rapidly if the pathogens are not sequestered or protected, such as by the biofilm. *Xoo* cells may produce some biofilm just after attachment, after which DSF production then enhances EPS and biofilm production. Subsequently, cells from this colony may leave to found new colonies further upstream in the xylem. Over 15 days, *Xoo* can progress 15-25 cm deep into the leaf, while the mutants lacking SWEET-inducing TALe progress only about 2-5 cm (PMID: 15553245). This progressive colonization model predicts that disease progression will be saltatory, *i.e*., that disease progression is initially not contiguous along the xylem walls, but through formation of distinct colonies. This hypothesis is testable using *Xoo* carrying a fluorescent protein or by visualizing local SWEET accumulation at the sites of successful infection. Other aspects of the model can be tested using host plants or *Xoo* cells that express genetically encoded sucrose sensors, or even sensors or reporters for quorum sensing. It may also be interesting to modulate individual components described here to determine the relative quantitative contribution of the individual factors. While editing of the three *SWEET* gene promoters currently holds promise for a robust, broad-spectrum resistance mechanism, a careful analysis of disease mechanics may provide important insights that will help to defeat new isolates that can overcome the broad spectrum SWEET-based resistance.

Residual low-level virulence of sux mutants

Clip infection uses high bacterial titers for inoculation and thus is not comparable to natural infections which likely require only a few bacteria to cause disease. The residual virulence observed here may therefore not be relevant in a natural environment. Notwithstanding, the *sux* mutant of PXO99^{A} still shows moderate virulence in clip infection assays, while PXO99^{A} strains lacking the TALe PthXo1, which induces *SWEET11a*, is avirulent. The *sux* mutant is likely still able to use some sucrose as a nutrient source or as a signal. It will thus be necessary to identify alternative uptake pathways, possibly via extracellular invertases derived from the host or enzymes derived from the bacteria that sustain this residual virulence.

Sucrose uptake and utilization by Xoo

When grown on minimal medium, growth of the Δ*sux* mutant is substantially impaired. Whether the remaining growth makes use of alternative low-capacity sucrose uptake or is due to the ability of *Xoo* to use glutamate and methionine in the medium as a carbon source remains to be determined. Yet even on full medium supplemented with sucrose, effective growth requires the *sux* gene cluster. Uptake into the cytosol of *Xoo* was measured using a genetically encoded biosensor. The Δ*suxC* mutant showed no detectable sucrose accumulation. With a K_d of 90 µM, the sensor has a linear response range *in vitro* between about 9 and 900 µM. Thus, if we assume that in PXO99^{A} the sensor is fully saturated, cytosolic levels exceed 900 µM in PXO99^{A} exposed to 10 mM sucrose. In the Δ*suxC* mutant sucrose levels remained below 9 µM. The recent development of ultrasensitive Matryoshka-type sensors may be useful to increase the sensitivity of the biosensors further and may enable analysis of sucrose levels in different compartments of the host and bacterial cells *in situ* with high temporal resolution.

Sucrose and hexoses as nutrients for Xoo

Previous reports had demonstrated that *Xoo*-triggered induction of at least one of the sucrose-specific transporters of plant is key to *Xoo* strain virulence in plant, while glucose-specific transporters do not show significant relationship with *Xoo* virulence (51). Thus, even if glucose can support growth and other virulence-related functions, sucrose must be the key player provided by the host. Nevertheless, *Xoo* is capable of using hexoses, which therefore could be derived from sucrose by extracellular enzymes such as apoplasmic invertases produced either by host or the bacteria. Notably, *Xoo* can grow on glucose as well. Xanthomonad genomes encode a large number of candidate hexose transporters (63). Mutants in the PTS glucose uptake system from *Xoo* for, which was essential for glucose uptake by *Xoo*, showed no effects on virulence (16). Hijacking of SWEETs is not unique to bacterial blight in rice but also occurs in bacterial blight of cotton and cassava (53,64). TAL_{Xam668} from *Xam* specifically induced the sucrose transporter gene *MeSWEET10a,* and virulence depends on the SWEET induction. Designer TAL effectors complemented the mutant phenotype of $TAL20_{Xam668}$, demonstrating that *MeSWEET10* is a susceptibility gene in cassava (53). Despite the similarity of the systems and the relatedness of the *Xanthomonas*

493 species, mutation of the *suxC* gene in *Xam* did not affect virulence. Indeed, *Xam*
494 infection led to increased mRNA levels of an apoplasmic invertase gene, which
495 could trigger extracellular hydrolysis of sucrose, followed by hexose uptake by
496 *Xam*, thereby feeding *Xam* indirectly with sucrose.

497 *Sucrose or its products as signals for transcriptional regulation*

498 Besides key roles in *Xoo* nutrition, sucrose also serves directly as a signal. SuxR
499 serves as a sucrose-specific receptor that derepresses the bidirectional pAB and
500 pC promoters to enable *Xoo* to use sucrose likely after invasion of the host. When
501 the *suxR* gene was deleted, sucrose uptake and hydrolysis were activated.
502 Whether SuxR can activate other target genes remains to be tested. Consistent
503 with the role in activation of sucrose utilization genes, Δ*suxR* mutants had no
504 substantial effect on growth or colony morphology, no effect on EPS levels, and
505 also did not impair virulence. Sucrose may also serve, directly or indirectly via
506 downstream metabolites as a signal that triggers quorum sensing (S9 Fig**)**.
507 Consistent with this hypothesis, DSF was able to supplement the EPS production
508 in the *sux* mutants. This hypothesis is testable, either by measuring the level of
509 DSF and BDSF levels in the presence or absence of sucrose, or by developing
510 biosensors that enable monitoring quorum-sensing factors during the infection with
511 spatial resolution.

512 *A possible role for sucrose in sensitizing Xoo to the quorum sensing factor DSF*

513 The sensitivity of the bacteria to quorum sensing factors can be modulated by
514 changing the receptor levels, e.g., for the *N*-acylated l-homoserine lactone
515 (AHL) sensing system TraR in *Agrobacterium tumefaciens*, LuxR in *Vibrio harveyi*,
516 LasR and QscR in *Pseudomonas aeruginosa* and RhlR in *E. coli* (65–68). Here we
517 found that, while transcripts for the rate limiting biosynthetic gene *rpfF* did not
518 increase when sucrose was added to Xoo cells, mRNA levels for the DSF receptor
519 histidine kinase *rpfC* and the di-cGMP cyclase *rpfG* increased. Glucose also
520 positively regulated *rpfC* and *G*, however to a much lower extend compared to
521 equimolar concentrations of sucrose. Importantly, *rpfC* and *G* transcript
522 abundance was also massively increased during infection, in parallel to that of *sux*
523 and *SWEET11a* genes. The sucrose-dependent increase may indicate that
524 bacteria are sensitized to quorum sensing factors when sucrose becomes
525 available due to PthXo1-triggered release of sucrose from host cells in the xylem.
526 Notably, at present, the interpretation of our data relies solely on transcriptional
527 effects, further experiments are required to measure sensitization more directly.
528 Also, the effect of mutations in the RpoN genes indicates that the regulatory
529 networks are more complex than described here (60); moreover
530 posttranscriptional regulations will also affect the response of the system (69).
531 Therefore, *Xoo* strains that lack the ability to induce host SWEET efflux activity
532 likely cannot trigger effective quorum sensing, and thus are less effective
533 swimmers and biofilm producers. Notably, transcripts of the key sigma factor σ^{54},
534 RpoN1 and RpoN2, and its downstream *gum* gene targets, which are responsible
535 for EPS production, were also sucrose inducible as shown here. Since RpoN1 and
536 RpoN2 do not appear to be involved in *rpfC* and *rpfG* regulation, the two pathways
537 may operate independently (60). Data obtained under SuxR derepression may

indicate a link between SuxR regulation and *RpoN* and *gum* genes, while regulation by sucrose of *rpf* genes seems be mediated by an independent mechanism. Taken together we propose a model in which pioneering *Xoo* manages enter the xylem, attach to the xylem parenchyma cells and inject TAL effectors into the host cells via a T3SS. A TALe like PthXo1 then binds to a *SWEET* promoter and activates transcription and production of a host plasma membrane sucrose uniporter like SWEET11a. Sucrose is released from the host cells along a concentration gradient and is then taken up by the Sux transporters into the cytosol of *Xoo*, where feedforward regulatory circuitry mediated by SuxR further enhances uptake (Fig 7). Sucrose or its degradation products, or the energy status trigger sensitization for quorum sensing factors important for further colonization of the xylem, as well as enhanced swimming and swarming capacity and EPS production via induction of σ^{54} factors. In particular it is possible that, as a result of the sucrose availability to *Xoo* cells, the quorum sensing machinery is sensitized by increased receptor density and cyclase activity to launch a successful attach. By contrast, when sucrose levels are low, flux through QS signaling is too low, thereby preventing efficient colonization by strains that cannot induce host SWEETs.

Regulatory networks

The regulatory network that controls virulence is highly complex and involves at least five parallel two component systems (TCS), of which the Rfp system is responsible for perception of DSF input that affect PDE activity and thus c-di-GMP levels (70). In turn, c-di-GMP levels differentially affect individual processes that relate to virulence via 4 parallel pathways (70). Notably, both transcriptional and translational regulation contribute to control (70). While our data may indicate that sucrose or a downstream signal could affect the DSF input into c-di-GMP signaling and affect multiple virulence aspects, it will be interesting to explore the role of sucrose on the other input and the out pathways. Notably, RfpE appears to not only play a role in swarming motility EPS production and virulence, but also be part of a feedback loop that impacts sucrose utilization (71).

New questions arising

It will be interesting to unravel the nature of the signal that triggers transcriptional activation of the core virulence genes. The regulatory networks involved appears to be extremely complex and will require extensive testing of the candidate targets identified in the *rpoN1* and *rpoN 2* mutants and the evaluation of posttranscriptional regulation (60,72). Ultimately, mathematical modeling will help to understand this complex network and help to explain why *Xoo* is so dependent on SWEET induction. While the order of events after attachment with respect to biofilm production appears obvious, it remains an open question how secreted DSF can be protected from dilution in the rapidly streaming xylem. This aspect is especially relevant regarding the possible role of DSF in swimming motility. Also, how *Xoo* can migrate against the xylem stream and dock at the lateral walls are important questions. We may be able to learn from studies in other systems, *e.g.*, Salmonella, which colonizes the intestinal lumen. Salmonella uses flagellar motility to get to the target cell surface, where physical forces lead to trapping for short

periods of time in a process termed 'near surface swimming' (73). In this mode the bacteria scan the cell surface and docking at areas with particular properties. These finding may help guiding research on *Xoo* swimming and docking.

Materials and Methods

Bacterial strains, plasmids, and DNA constructs

Strains of *Escherichia coli*, *Xoo* and plasmids used here are listed in S3 Table. Standard bacterial culture and DNA techniques were used for *E. coli* and recombinant DNA manipulations as previously described (74). Liquid and solid cultures of *Xoo* were grown at 28 °C in NBN (Difco nutrient broth: beef extract, 3.0 g; peptone, 5.0 g/L) and NAN (NB with agar 15 g/L) media, respectively. For analysis of sucrose dependence, a modified synthetic minimal medium (based on New Synthetic Medium (73), NSM: (g/L): sucrose (10); Na-glutamate (5); methionine (0.1); KH_2PO_4 (1); NH_4Cl (1); $MgCl_2 \cdot 6\ H_2O$ (1); and Fe-EDTA (1 ppm); MOPS (0.1 M); $CaCl_2$ (0.1 mM); pH 7.0) was used. Media were supplemented with sucrose, glucose or fructose at the mentioned concentrations. Antibiotics were added as follows: ampicillin (100 µg/mL), cephalexin (10 µg/mL), kanamycin (25 µg/mL for *Xoo*; 50 µg/mL for *E. coli*) and spectinomycin (100 µg/mL). *E. coli* and *Xoo* were transformed by electroporation.

Construction of sux mutants in PXO99^A

The in-frame deletion mutants of *sux* genes (Δ*sux*, Δ*suxA*, Δ*suxC*, Δ*suxB* and Δ*suxR*) in PXO99^A were constructed by homologous recombination and marker exchange as previously described (75) using primers listed in S1 Table. In brief, 5'- and 3'-flanking sequences of each *sux* gene were amplified by PCR from PXO99^A genomic DNA. The two PCR-amplicons were fused by overlap extension PCR and cloned into pGEM-T (Promega) by TA cloning. Constructs were verified by sequencing. This intermediate construct was then fused to a cassette containing the *sacB* gene and neomycin phosphotransferase gene in pKMS1sacB-Kn (76) to produce the suicide vectors used to knockout the genes of interest. PXO99^A was transformed with pKMS1 constructs by electroporation. Transformants were plated on selective NA medium containing kanamycin. Single colonies were transferred to liquid NB medium supplemented with 10 % sucrose and grown for 12 h at 28 °C, before plating on NA medium supplemented with 10 % sucrose. Single sucrose-tolerant colonies were used to inoculate both solid NA and NA-containing kanamycin. Sucrose-tolerant and kanamycin-sensitive (tested as replicates) colonies were putative deletion mutants. The deletions were confirmed by PCR amplification using primers located outside the homologous regions used for marker exchange mutagenesis. Deletions were confirmed by comparing PCR product length. Two independent sets of deleted strains were generated in two different locations. Both sets gave comparable results for at least some phenotypes, demonstrating that the observed phenotypes are not caused by artifacts due to mutant selection on 10 % sucrose. Fig 1a, 2, 3 and 4 contain data from one set of mutants while Fig 1b and 6 contain data from an independent set.

Construction of sux genes for functional complementation of sux mutants

Functional complementation was performed using primers listed in S4 Table. Expression of *suxA*, *suxR*, *suxB* and *suxC* were made by cloning either the *lacZ* promoter or native promoters into the corresponding mutants. For *suxB*, the native promoter for the *suxAB* operon was fused to the *suxB* coding sequence by overlap extension PCR. All nucleotide sequences were amplified by PCR from PXO99^{A} genomic DNA and cloned into pGEM-T (Promega). These intermediate constructs were verified by sequencing. Coding regions with or without promoter regions were subcloned into pHM1 containing the *lacZ* promoter (77). The Δ*suxA*, Δ*suxB*, Δ*suxC*, and Δ*suxR* strains were each used as the recipients for the above recombinant plasmids. Transformants harboring the recombinant plasmids were selected on solid NA plates with appropriate antibiotics. Complemented strains were confirmed by PCR amplification with the corresponding gene-specific primer pairs.

OD_{600} and CFU/mL measurements

OD_{600} was used as a proxy for bacterial growth either using a plate reader (*e.g.*, growth curves) or a spectrophotometer. The corresponding CFU/mL was determined (S6 Table).

RNA isolation and quantitative RT-PCR from Xoo cells from in vitro culture medium

Cells from *in vitro* cultures (OD_{600} ~2.0 for stationary phase or as specified for 2, 4, 6 and 8 hours of bacterial growth (S11 Fig.)) were harvested and washed twice with sterile water prior to RNA extraction. Total bacterial RNA was extracted using TRIZOL (Invitrogen, Carlsbad, CA, USA) according to manufacturer's instructions. Total RNA (1 µg) was treated with DNase I (Thermo Scientific, Carlsbad, CA, USA) and used for cDNA synthesis using iScript cDNA Synthesis (Bio-Rad Laboratories, USA). cDNA derived from 25 ng of total RNA was used for each quantitative real-time PCR (qRT-PCR) reaction with gene-specific primers listed in S4 Table. Ribosomal 16S RNA expression was used as an internal control. The qRT-PCR was performed on a Stratagene Mx4000 multiplex quantitative PCR system using iQSYBRGreenSupermix (Bio-Rad, Hercules, USA). The average cycle threshold (Ct) was used to determine candidate gene transcript levels. The $2^{-\Delta\Delta}$Ct method was used for relative quantification using 16S rRNA as reference. The Ct values of 16S rRNA were in a similar range as those of the candidate genes (S5 Table), and the reference gene 16S rRNA has also been used in other studies (78).
qRT-PCR was performed and transcript level was determined relative to 16S rRNA. For *in vitro* data, transcript levels were then normalized to the control, and the control value was shown (at 1 for PXO99^{A} no sugar) with errors and the data in the mutants or in presence of sugar. For *in planta* data, transcript levels were then normalized to the control, and the control value was shown (for 0 day) with errors and the data at 3, 5, 7 and 10 days.

RNA isolation and quantitative RT-PCR from Xoo cells from rice leave

Four-week-old rice plants, cv. Kitaake, were inoculated by clipping the leaf tips with scissors dipped in bacterial suspension (OD_{600} ~0.5). Infected rice plants were kept in a growth chamber under 12-h light at 28 °C and 12-h dark at 25 °C. Leaf segments (3 cm) were collected at 0, 3, 5, 7 and 10 days after infection (DAI). Total RNA was extracted using TRIZOL (Invitrogen, Carlsbad, CA, USA) according to manufacturer's instructions. Total RNA (1 µg) was treated with DNase I (Thermo Scientific, Carlsbad, CA, USA) and used for cDNA synthesis using Maxima™ H Minus cDNA Synthesis Master Mix, with dsDNase (Thermo Scientific, Carlsbad, CA, USA). cDNA derived from 25 ng of total RNA was used for each quantitative real-time (qRT-PCR) reaction with gene-specific primers listed in S4 Table. Ribosomal 16S RNA expression was used as an internal control with the gene-specific primers. The qRT-PCR was performed on Applied Biosystems 7500/7500 Fast Real-Time PCR System(Applied Biosystems, USA) using SYBR Fast Universal kit (Kapa Biosystems). The average threshold cycle (Ct) was used to determine the gene expression. The $2^{-\Delta\Delta}$Ct method was used for relative quantification (78).

Observation of bacterial colony morphology and quantification of EPS

Deletion mutants and wild-type $PXO99^{A}$ were grown on solid NA medium (plates were not inverted) and resuspended into liquid NB media to an OD_{600} ~0.2, then 2 µL of the bacterial suspension was dropped on solid medium with or without added sugars as specified for spot assays. Bacterial colonies were photographed after 2, 3, 4, 5 or 7 days at 28 °C as specified and phenotype of colonies was recorded by vertical photography. Colony morphology was also assessed by recording the colony cohesion when bacteria were grown on inverted plates. Droplet formation indicated reduced EPS production. Phenotype of colonies was recorded by horizontal photography. EPS was quantified as previously described (79). Briefly, 10-mL bacterial cultures were grown in liquid NB with or without added sugar for 2 days at 28 °C. At OD_{600} ~2.3, cells were harvested by centrifugation (8,000 *g* for 10 min). KCl solution (400 µL, 3.4 M) was added to the supernatants followed by 2 volumes of absolute ethanol. The mixture was incubated at -20 °C for 30 minutes. The precipitated EPS was harvested by centrifugation (10,000 *g* for 10 min) and dried at 55 °C overnight before measuring weights. DSF supplementation was performed by adding with 5 µM of *cis*-11-methyl-2-dodecenoic acid (Sigma) to the media.

Determination of bacterial growth

Bacteria were grown in 96-well, flat-bottom, transparent plates with 200 µL of liquid NB or minimal media and inoculated with *Xoo* at OD_{600} ~0.15. Non-inoculated wells were used for background subtraction. The OD_{600} was measured every 30 min for 2 days at 28 °C using a plate reader (Tecan). Prior to measurements cells were mixed by shaking for 5 seconds.

Sucrose uptake into Xoo using FRET sensors

Xoo cultures were transformed by electroporation with a plasmid encoding FLIPsuc-90µΔ1V (ref. (56)) under the control of the neomycin promoter. *Xoo* cells were grown for 2-3 days at 28-30 °C in solid media containing antibiotics for

selection. Single colonies were used to inoculate 5 mL TS medium (10 g tryptone, 1g glutamic acid and 10 g sucrose per liter) containing the appropriate antibiotic. *Xoo* transformants were grown for 2 days at 28-30 °C. The 5-mL cultures were used to inoculate 100 mL liquid TS medium containing the appropriate antibiotic. At OD_{600} ~0.3-0.4, the cells were harvested by centrifugation (3,000 *g* for 10 min) and the cell pellets were resuspended in M9 medium (0.1 M MOPS, 1 mM $MgSO_4$, 1 mM $CaCl_2$, 0.1 % NH_4Cl, 0.05 % NaCl, 0.3 % KH_2PO_4, 0.6 % Na_2HPO_4) to OD_{600} ~1.3-1.4. eCFP and eYFP fluorescence intensity was recorded in a 96-well, flat-bottom transparent plate (excitation 428 and 505 nm; emission at 470 and 535 nm) using a fluorometer microplate reader (Tecan Spark, Männedorf Switzerland). Kinetic experiments were performed by measuring 5 initial cycles without sucrose followed by 5 cycles after addition of 2 µL of 1 M sucrose to 200 µL of the cell suspensions (*i.e.,* final concentrations of 10 mM sucrose). Non-transformed *Xoo* cells were used to subtract cell-specific background in subsequent data analyses.

Swimming motility assays

Motility assays were conducted on soft agar (0.3 %, w/v) essentially as described (80). *Xoo* cells were grown in liquid NB at 28 °C and 2 µL of culture (0.1 OD_{600}) was dropped on solid NA with 1 % sucrose. The diameters of the swimming motility zones were measured after incubation at 28 °C on uninverted plates for 1, 2, 3, 5 and 7 days as specified and phenotype of colonies was recorded by vertical photography.

Swarming motility assays

Motility assays were undertaken on 0.6 % agar (w/v). *Xoo* cells were grown on liquid NB at 28 °C and 2 µL of culture (0.1 OD_{600}) was dropped onto plate containing NA with 1 % sucrose. The diameters of the swarming motility zones were measured after incubation at 28 °C on uninverted plates for 1, 2, 3, 5 and 7 days as specified and phenotype of colonies was recorded by vertical photography.

Analysis of biofilm formation

Biofilm formation and quantification assays were performed by growing *Xoo* to logarithmic phase. 5 mL of culture (0.1 OD_{600}) was then incubated at 28 °C for 72 h in static glass tubes (qualitative assays) or 96-well, flat-bottom transparent plates (quantitative assays). Medium and cells in solution were removed and the biofilm component was washed twice with water and stained with 0.1 % crystal violet (CV, w/v) solution for 48 h. Stained biofilms were further washed three times with water. Pictures were taken (glass tubes) or crystal violet amounts were quantified (96-well plates). For quantification, the bound crystal violet was dissolved in ethanol and read at 595 nm (absorbance maximum of crystal violet) with a microplate reader (Tecan Spark).

Disease assays in rice leaves

The *japonica* rice cv. Nipponbare was grown in a chamber under a cycle of 12 h of light at 28 °C and 12 h of dark at 25 °C. Four-week-old rice plants were

inoculated with bacterial suspensions in sterile distilled water at approximately OD_{600} ~0.5 using leaf tip-clipping. Lesion lengths were measured 12 DAI (81).

Building of the phylogenic tree of the sux gene cluster

Prior to phylogenetic tree construction, the *sux* coding sequences were artificially condensed following the same vectorial orientation, namely *suxR*, *suxC*, *suxA* and *suxB*. This analysis was done to roughly estimate the conservation of the *sux* gene cluster in *Xanthomonas* spp. Given the variability of the intergenic region, the condensed DNA sequences of the *sux* cluster were artificially generated. The phylogenetic tree was inferred from the condensed *sux* gene cluster sequences of 14 *Xanthomonas* spp.: *X. arboricola* pv. *juglandis, X. citri* pv. *malvacearum, X. vasicola* pv. *vasculorum, X. cucurbitae, X. phaseoli, X. oryzae* pv. *oryzicola, X. oryzae* pv. *oryzae, X. hortorum, X. fragariae, X. campestris* pv. *vesicatoria, X. vesicatoria, X. campestris* pv. *campestris, X. translucens* pv. *translucens,* and *X. albilineans*. The unweighted pair group method with arithmetic mean (UPGMA) (Mitchener & Sokal 1957) was used and based on the Tamura-Nei model. The tree was calculated from a global alignment performed from pairwise alignment of all sequence pairs using Geneious (https://www.geneious.com/).

Statistics

In all experiments, at minimum, three independent experiments were performed with three biological replicates each. Significance was calculated between two groups using unpaired two-tailed Student's *t*-Test at the 95 % confidence level and Welch's correction of unequal variances. For infection experiments, at least 7 leaves from five plants were used per strain.

Figure preparation

Some figure sections were generated with Biorender (https://biorender.com).

Acknowledgments

We would like to thank Boris Szurek for advising the Frommer team on *Xoo* transformation. We would like to thank Susanne Paradies for excellent technical assistance. This work was supported by grants from the Bill and Melinda Gates Foundation to HHU (WF), with a subcontract to MU (BY), the Deutsche Forschungsgemeinschaft (DFG, German Research Foundation) under Germany´s Excellence Strategy – EXC-2048/1 – project ID 390686111, and the Alexander von Humboldt Professorship (WF). YA is supported by a fellowship from the Alexander von Humboldt Foundation.

Funding statement

The work presented here was supported by: WF: project ID 390686111 (Bill and Melinda Gates Foundation; www.gatesfoundation.org), project ID 390686111 (Deutsche Forschungsgemeinschaft, German Research Foundation under Germany´s Excellence Strategy EXC-2048/1; www.dfg.de), (Alexander von Humboldt Professorship; www.humboldt-foundation.de). BY: project ID 390686111 (subcontract to HHU, funds from Bill and Melinda Gates Foundation). YA: Fellowship (Alexander von Humboldt fellowship). The funders had no role in

study design, data collection and analysis, decision to publish, or preparation of the manuscript.

References

1. Savary S, Willocquet L, Pethybridge SJ, Esker P, McRoberts N, Nelson A. The global burden of pathogens and pests on major food crops. Nat Ecol Evol. 2019;3(3):430–9.
2. Shekhar S, Sinha D, Kumari A. An Overview of bacterial leaf blight disease of rice and different strategies for its management. Int J Curr Microbiol App Sci. 2020;9(4):2250–65.
3. Ou SH. Rice diseases. IRRI; 1985.
4. McCully ME. Niches for bacterial endophytes in crop plants: a plant biologist's view. Funct Plant Biol. 2001;28(9):983–90.
5. Peuke AD, Rokitta M, Zimmermann U, Schreiber L, Haase A. Simultaneous measurement of water flow velocity and solute transport in xylem and phloem of adult plants of *Ricinus communis* over a daily time course by nuclear magnetic resonance spectrometry. Plant Cell Environ. 2001;24(5):491–503.
6. Tyree MT, Zimmermann MH. Xylem structure and the ascent of sap. Springer Science & Business Media; 2013.
7. Lowe-Power TM, Khokhani D, Allen C. How *Ralstonia solanacearum* exploits and thrives in the flowing plant xylem environment. Trends Microbiol. 2018 Nov;26(11):929–42.
8. Dalsing BL, Truchon AN, Gonzalez-Orta ET, Milling AS, Allen C. Ralstonia solanacearum uses inorganic nitrogen metabolism for virulence, ATP production, and detoxification in the oxygen-limited host xylem environment. MBio. 2015;6(2):e02471-14.
9. Lowe-Power TM, Khokhani D, Allen C. How *Ralstonia solanacearum* exploits and thrives in the flowing plant xylem environment. Trends Immunol. 2018;26(11):929–42.
10. Jacobs JM, Babujee L, Meng F, Milling A, Allen C. The *in planta* transcriptome of *Ralstonia solanacearum*: conserved physiological and virulence strategies during bacterial wilt of tomato. MBio. 2012;3(4):e00114-12.
11. Bogs J, Geider K. Molecular analysis of sucrose metabolism of *Erwinia amylovora* and influence on bacterial virulence. J Bacteriol. 2000;182(19):5351–8.
12. Hamilton CD, Steidl OR, MacIntyre AM, Hendrich CG, Allen C. *Ralstonia solanacearum* depends on catabolism of myo-inositol, sucrose, and trehalose for virulence in an infection stage-dependent manner. Mol Plant-Microbe Interact. 2021;(ja).
13. Yadeta K, Thomma B. The xylem as battleground for plant hosts and vascular wilt pathogens. Front Plant Sci [Internet]. 2013 [cited 2021 Mar 17];4. Available from: https://www.frontiersin.org/articles/10.3389/fpls.2013.00097/full
14. Noda T, Kaku H. Growth of *Xanthomonas oryzae* pv. *oryzae in planta* and in guttation fluid of rice. Jap J Phytopathol. 1999;65(1):9–14.
15. Wang J, Guo J, Wang S, Zeng Z, Zheng D, Yao X, et al. The global strategy employed by *Xanthomonas oryzae* pv. *oryzae* to conquer low-oxygen tension. J Proteomics. 2017;161:68–77.
16. Tsuge S, Nishida M, Furutani A, Yasuyuki K, Horino O. Growth of glucose-uptake-deficient mutant of *Xanthomonas oryzae* pv. *oryzae* in rice leaves. J Gen Plant

Pathol. 2001;67(2):144–7.
17. Eom J-S, Luo D, Atienza-Grande G, Yang J, Ji C, Huguet-Tapia JC, et al. Diagnostic kit for rice blight resistance. Nat Biotechnol. 2019;37(11):1372–9.
18. Meng Y, Li Y, Galvani CD, Hao G, Turner JN, Burr TJ, et al. Upstream migration of *Xylella fastidiosa* via pilus-driven twitching motility. J Bacteriol. 2005;187(16):5560–7.
19. Yang B, White FF. Diverse members of the AvrBs3/PthA family of type III effectors are major virulence determinants in bacterial blight disease of rice. Mol Plant Microbe Interact. 2004;17(11):1192–200.
20. Yang B, Sugio A, White FF. *Os8N3* is a host disease-susceptibility gene for bacterial blight of rice. Proc Natl Acad Sci USA. 2006 Jul 5;103(27):10503–8.
21. Kay S, Bonas U. How *Xanthomonas* type III effectors manipulate the host plant. Curr Opin Microbiol. 2009 Feb 1;12(1):37–43.
22. Zhou J, Peng Z, Long J, Sosso D, Liu B, Eom J-S, et al. Gene targeting by the TAL effector PthXo2 reveals cryptic resistance gene for bacterial blight of rice. Plant J. 2015;82(4):632–43.
23. Kharadi RR, Sundin GW. Dissecting the process of xylem colonization through biofilm formation in *Erwinia amylovora*. J Plant Pathol. 2020;1–9.
24. Iyer R, Camilli A. Sucrose metabolism contributes to in vivo fitness of *Streptococcus pneumoniae*. Mol Microbiol. 2007;66(1):1–13.
25. Lee B-M, Park Y-J, Park D-S, Kang H-W, Kim J-G, Song E-S, et al. The genome sequence of *Xanthomonas oryzae* pathovar oryzae KACC10331, the bacterial blight pathogen of rice. Nucl Acids Res. 2005;33(2):577–86.
26. He Y-W, Wu J, Cha J-S, Zhang L-H. Rice bacterial blight pathogen *Xanthomonas oryzae* pv. *oryzae* produces multiple DSF-family signals in regulation of virulence factor production. BMC Microbiol. 2010;10(1):1–9.
27. Devos S, Van Oudenhove L, Stremersch S, Van Putte W, De Rycke R, Van Driessche G, et al. The effect of imipenem and diffusible signaling factors on the secretion of outer membrane vesicles and associated Ax21 proteins in *Stenotrophomonas maltophilia*. Front Microbiol. 2015;6:298.
28. Loh J, Pierson EA, Pierson III LS, Stacey G, Chatterjee A. Quorum sensing in plant-associated bacteria. Curr Opin Plant Biol. 2002;5(4):285–90.
29. Ryan RP, An S, Allan JH, McCarthy Y, Dow JM. The DSF family of cell–cell signals: an expanding class of bacterial virulence regulators. PLoS Pathog. 2015;11(7):e1004986.
30. Emge P, Moeller J, Jang H, Rusconi R, Yawata Y, Stocker R, et al. Resilience of bacterial quorum sensing against fluid flow. Scientific Reports. 2016;6(1):1–10.
31. Samal B, Chatterjee S. New insight into bacterial social communication in natural host: Evidence for interplay of heterogeneous and unison quorum response. PLoS genetics. 2019;15(9):e1008395.
32. Zheng D, Yao X, Duan M, Luo Y, Liu B, Qi P, et al. Two overlapping two-component systems in *Xanthomonas oryzae* pv. *oryzae* contribute to full fitness in rice by regulating virulence factors expression. Sci Rep. 2016;6(1):1–13.
33. Killiny N, Martinez RH, Dumenyo CK, Cooksey DA, Almeida RPP. The exopolysaccharide of *Xylella fastidiosa* Is essential for biofilm formation, plant virulence, and vector transmission. Mol Plant Microbe Interact. 2013 Sep 1;26(9):1044–53.

34. Danhorn T, Fuqua C. Biofilm formation by plant-associated bacteria. Annu Rev Microbiol. 2007;61:401–22.
35. Koczan JM, McGrath MJ, Zhao Y, Sundin GW. Contribution of *Erwinia amylovora* exopolysaccharides amylovoran and levan to biofilm formation: implications in pathogenicity. Phytopathol. 2009 Nov;99(11):1237–44.
36. Katzen F, Ferreiro DU, Oddo CG, Ielmini MV, Becker A, Pühler A, et al. *Xanthomonas campestris pv. campestris* gum mutants: Effects on xanthan biosynthesis and plant virulence. J Bacteriol. 1998 Apr;180(7):1607–17.
37. Hunjan MS, Singh PP, Lore JS. Extracellular polysaccharide production underlining aggressiveness of *Xanthomonas oryzae* pv. *oryzae* infecting rice. Indian Phytopathol. 2015;68(1):120–2.
38. Dharmapuri S, Sonti RV. A transposon insertion in the gumG homologue of *Xanthomonas oryzae* pv. *oryzae* causes loss of extracellular polysaccharide production and virulence. FEMS Microbiol Lett. 1999;179(1):53–9.
39. Triplett LR, Hamilton JP, Buell CR, Tisserat NA, Verdier V, Zink F, et al. Genomic analysis of *Xanthomonas oryzae* isolates from rice grown in the United States reveals substantial divergence from known *X. oryzae* pathovars. Appl Environ Microbiol. 2011;77(12):3930–7.
40. Oliva R, Ji C, Atienza-Grande G, Huguet-Tapia JC, Perez-Quintero A, Li T, et al. Broad-spectrum resistance to bacterial blight in rice using genome editing. Nat Biotechnol. 2019;37(11):1344–50.
41. Jeena GS, Kumar S, Shukla RK. Structure, evolution and diverse physiological roles of SWEET sugar transporters in plants. Plant Mol Biol. 2019 Jul 1;100(4):351–65.
42. Zaka A, Grande G, Coronejo T, Quibod IL, Chen C-W, Chang S-J, et al. Natural variations in the promoter of *OsSWEET13* and *OsSWEET14* expand the range of resistance against *Xanthomonas oryzae* pv. *oryzae*. Sundaram RM, editor. PLoS one. 2018 Sep 13;13(9):e0203711.
43. Chen L-Q, Hou B-H, Lalonde S, Takanaga H, Hartung ML, Qu X-Q, et al. Sugar transporters for intercellular exchange and nutrition of pathogens. Nature. 2010;468(7323):527.
44. Chen L-Q. SWEET sugar transporters for phloem transport and pathogen nutrition. New Phytol. 2014;201(4):1150–5.
45. Chandran D. Co-option of developmentally regulated plant SWEET transporters for pathogen nutrition and abiotic stress tolerance. IUBMB life. 2015;67(7):461–71.
46. Yu Y, Streubel J, Balzergue S, Champion A, Boch J, Koebnik R, et al. Colonization of rice leaf blades by an African strain of *Xanthomonas oryzae* pv. *oryzae* depends on a new TAL effector that induces the rice nodulin-3 Os11N3 gene. Mol Plant Microbe Interact. 2011;24(9):1102–13.
47. Oliva R, Ji C, Atienza-Grande G, Huguet-Tapia JC, Pérez-Quintéro A, Li T, et al. Broad-spectrum resistance to bacterial blight in rice using genome-editing. Nat Biotechnol. 2019;37:1344–50.
48. Eom J-S, Luo D, Atienza-Grande G, Yang J, Ji C, Luu VT, et al. Diagnostic kit for rice blight resistance. Nat Biotechnol. 2019;37:1372–9.
49. Bezrutczyk M, Yang J, Eom J-S, Prior M, Sosso D, Hartwig T, et al. Sugar flux and signaling in plant-microbe interactions. Plant J. 2018 Feb;93(4):675–85.
50. Streubel J, Pesce C, Hutin M, Koebnik R, Boch J, Szurek B. Five

phylogenetically close rice *SWEET* genes confer TAL effector-mediated susceptibility to *Xanthomonas oryzae pv. oryzae*. New Phytol. 2013;200(3):808–19.

51. Blanvillain S, Meyer D, Boulanger A, Lautier M, Guynet C, Denancé N, et al. Plant carbohydrate scavenging through TonB-dependent receptors: a feature shared by phytopathogenic and aquatic bacteria. PLoS one. 2007;2(2):e224.

52. Kim H-S, Park H-J, Heu S, Jung J. Molecular and functional characterization of a unique sucrose hydrolase from *Xanthomonas axonopodis* pv. *glycines*. J Bacteriol. 2004;186(2):411–8.

53. Cohn M, Bart RS, Shybut M, Dahlbeck D, Gomez M, Morbitzer R, et al. *Xanthomonas axonopodis* virulence is promoted by a transcription activator-like effector–mediated induction of a SWEET sugar transporter in cassava. Mol Plant Microbe Interact. 2014;27(11):1186–98.

54. Novichkov PS, Laikova ON, Novichkova ES, Gelfand MS, Arkin AP, Dubchak I, et al. RegPrecise: a database of curated genomic inferences of transcriptional regulatory interactions in prokaryotes. Nucleic Acids Res. 2010;38(suppl_1):D111–8.

55. Yuan W. Culture medium for *Xanthomonas campestris* pv. *oryzae*. J Appl Microbiol. 1990;69(6):798–805.

56. Lager I, Looger LL, Hilpert M, Lalonde S, Frommer WB. Conversion of a putative *Agrobacterium* sugar-binding protein into a FRET sensor with high selectivity for sucrose. J Biol Chem. 2006 Oct 13;281(41):30875–83.

57. Liu A, Mi Z-H, Zheng X-Y, Yu Y, Su H-N, Chen X-L, et al. Exopolysaccharides play a role in the swarming of the benthic bacterium *Pseudoalteromonas* sp. SM9913. Frontiers in microbiology. 2016;7:473.

58. Wang X-Y, Zhou L, Yang J, Ji G-H, He Y-W. The RpfB-dependent quorum sensing signal turnover system is required for adaptation and virulence in rice bacterial blight pathogen *Xanthomonas oryzae* pv. *oryzae*. Mol Plant Microbe Interact. 2016;29(3):220–30.

59. Yang F, Tian F, Chen H, Hutchins W, Yang C-H, He C. The *Xanthomonas oryzae* pv. *oryzae* PilZ domain proteins function differentially in cyclic di-GMP binding and regulation of virulence and motility. Applied and environmental microbiology. 2015;81(13):4358–67.

60. Yu C, Nguyen D-P, Yang F, Shi J, Wei Y, Tian F, et al. Transcriptome Analysis Revealed Overlapping and Special Regulatory Roles of RpoN1 and RpoN2 in Motility, Virulence, and Growth of *Xanthomonas oryzae* pv. *oryzae*. Front Microbiol. 2021;12:453.

61. Dharmapuri S, Sonti RV. A transposon insertion in the *gumG* homologue of *Xanthomonas oryzae* pv. *oryzae* causes loss of extracellular polysaccharide production and virulence. FEMS Microbiol Lett. 1999;179(1):53–9.

62. Tyree MT, Zimmermann MH. Xylem structure and the ascent of sap. 2nd ed. Berlin ; New York: Springer-Verlag; 2002. 283 p. (Springer series in wood science).

63. Jahreis K, Bentler L, Bockmann J, Hans S, Meyer A, Siepelmeyer J, et al. Adaptation of sucrose metabolism in the *Escherichia coli* wild-type strain EC3132. J Bacteriol. 2002;184(19):5307–16.

64. Cox KL, Meng F, Wilkins KE, Li F, Wang P, Booher NJ, et al. TAL effector driven induction of a *SWEET* gene confers susceptibility to bacterial blight of cotton. Nat Commun. 2017;8(1):1–14.

65. Zhu J, Beaber JW, Moré MI, Fuqua C, Eberhard A, Winans SC. Analogs of the autoinducer 3-oxooctanoyl-homoserine lactone strongly inhibit activity of the TraR protein of *Agrobacterium tumefaciens*. J Bacteriol. 1998 Oct;180(20):5398–405.
66. Collins CH, Arnold FH, Leadbetter JR. Directed evolution of *Vibrio fischeri* LuxR for increased sensitivity to a broad spectrum of acyl-homoserine lactones. Mol Microbiol. 2005;55(3):712–23.
67. Moore JD, Rossi FM, Welsh MA, Nyffeler KE, Blackwell HE. A comparative analysis of synthetic quorum sensing modulators in *Pseudomonas aeruginosa*: new insights into mechanism, active efflux susceptibility, phenotypic response, and next-generation ligand design. J Am Chem Soc. 2015 Nov 25;137(46):14626–39.
68. Wellington S, Greenberg EP. Quorum sensing signal selectivity and the potential for interspecies cross talk. mBio. 2019 Mar 5;10(2):e00146-19.
69. Cheng Z, He Y-W, Lim SC, Qamra R, Walsh MA, Zhang L-H, et al. Structural basis of the sensor-synthase interaction in autoinduction of the quorum sensing signal DSF biosynthesis. Structure. 2010;18(9):1199–209.
70. Yang F, Xue D, Tian F, Hutchins W, Yang C-H, He C. Identification of c-di-GMP signaling components in *Xanthomonas oryzae* and their orthologs in Xanthomonads involved in regulation of bacterial virulence expression. Front Microbiol. 2019;10:1402.
71. Cho J-H, Yoon J-M, Lee S-W, Noh Y-H, Cha J-S. *Xanthomonas oryzae* pv. *oryzae* RpfE regulates virulence and carbon source utilization without change of the dsf production. Plant Pathol J. 2013;29(4):364.
72. Samal B, Chatterjee S. New insight into bacterial social communication in natural host: Evidence for interplay of heterogeneous and unison quorum response. PLoS Genet. 2019;15(9):e1008395.
73. Misselwitz B, Barrett N, Kreibich S, Vonaesch P, Andritschke D, Rout S, et al. Near surface swimming of *Salmonella Typhimurium* explains target-site selection and cooperative invasion. PLoS Pathog. 2012;8(7):e1002810.
74. Ausubel FM, Brent R, Kingston RE, Moore DD, Seidman JG, Smith JA, et al. Current protocols in molecular biology. VB Chanda, series ed. New York: John Wiley & Sons; 1998.
75. Song C, Yang B. Mutagenesis of 18 type III effectors reveals virulence function of XopZ(PXO99) in *Xanthomonas oryzae* pv. *oryzae*. Mol Plant Microbe Interact. 2010;23(7):893–902.
76. Zhao S, Mo W-L, Wu F, Tang W, Tang J-L, Szurek B, et al. Identification of non-TAL effectors in *Xanthomonas oryzae* pv. *oryzae* Chinese strain 13751 and analysis of their role in the bacterial virulence. World J Microbiol Biotechnol. 2013;29(4):733–44.
77. Zou L, Li Y, Chen G. A non-marker mutagenesis strategy to generate poly-*hrp* gene mutants in the rice pathogen *Xanthomonas oryzae* pv. *oryzicola*. Agric Sci China. 2011 Aug 1;10(8):1139–50.
78. Livak KJ, Schmittgen TD. Analysis of relative gene expression data using real-time quantitative PCR and the 2− ΔΔCT method. Methods. 2001;25(4):402–8.
79. Amikam D, Galperin MY. PilZ domain is part of the bacterial c-di-GMP binding protein. Bioinformatics. 2006;22(1):3–6.
80. González JF, Myers MP, Venturi V. The inter-kingdom solo OryR regulator of *Xanthomonas oryzae* is important for motility. Mol Plant Pathol. 2013;14(3):211–21.
81. Kauffman HE. An improved technique for evaluating resistance of rice varieties

to *Xanthomonas oryzae*. Plant Dis Rep. 1973;57:537–41.

82. Slater H, Alvarez-Morales A, Barber CE, Daniels MJ, Dow JM. A two-component system involving an HD-GYP domain protein links cell–cell signalling to pathogenicity gene expression in *Xanthomonas campestris*. Mol Microbiol. 2000;38(5):986–1003.

83. Azimi S, Klementiev AD, Whiteley M, Diggle SP. Bacterial quorum sensing during infection. Annu Rev Microbiol. 2020;74:201–19.

Figures and Tables

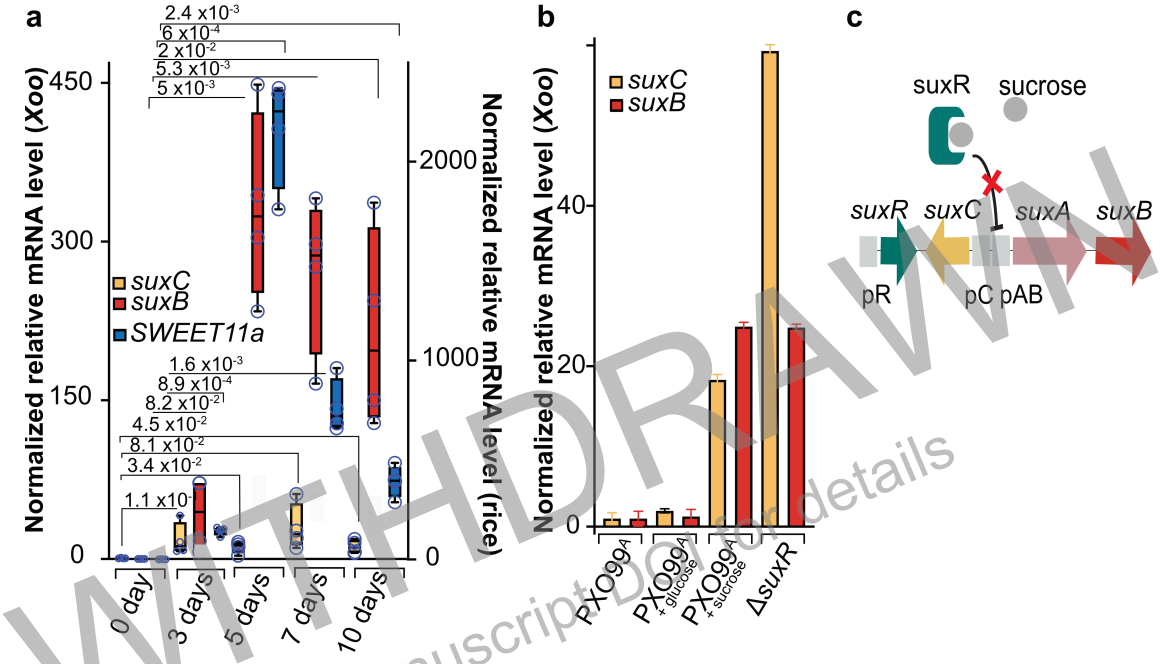

Figure 1. Transcript levels of *Sux* genes *in vitro* and *in planta* and role of the repressor SuxR. a. *sux* transcript levels in PXO99^{A} and *SWEET11a* in rice during infection of rice cultivar Kitaake as determined by qRT-PCR (0, 3, 5, 7 and 10 days after infection in Kitaake). **b.** qRT-PCR analyses of *suxB* and *suxC* mRNA levels in *Xoo* growing on NBN, NBN + 1 % sucrose and NBN + 1 % glucose and in presence or absence of SuxR repression (Δ*suxR*). **c.** Proposed model of regulation of *suxC* and *suxB* by SuxR. Boxes extend from 25th to 75th percentiles and display median values as center lines. Whiskers plot minimum and maximum values and individual data points. Significance was calculated between two groups using unpaired two-tailed Student's *t*-Test at the 95 % confidence level and Welch's correction of unequal variances. The $2^{-\Delta\Delta}$Ct method was used for relative quantification using 16S rRNA as reference. Transcript levels were then normalized to the control, and the control value was shown (at 1 PXO99^{A} no sugar for *in vitro* and 0 day for *in planta*). Comparable results were obtained in three independent experiments. See also S1, S2 and S3 Figures.

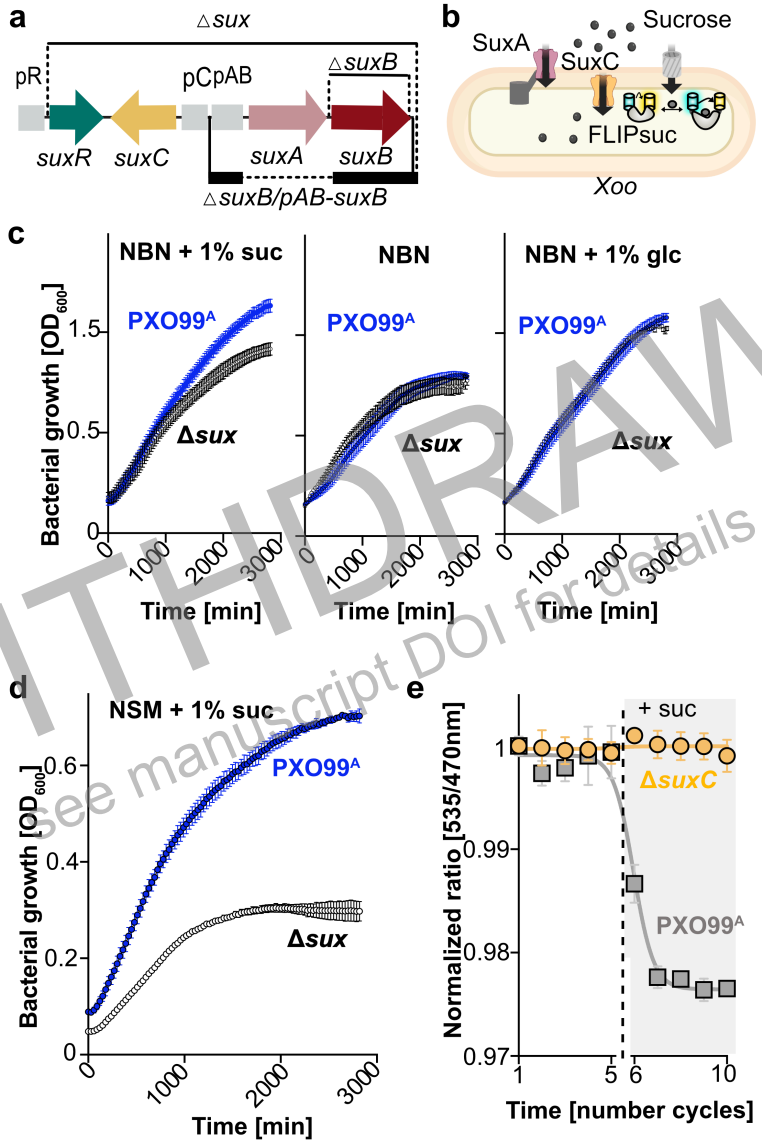

Figure 2. Effect of mutations in *sux* genes on bacterial growth and sucrose uptake as measured with a sucrose FRET sensor. a. Illustration of deletions used in this study **b.** Illustration of *Xoo* expressing the FLIPsuc-90μΔ1V with an unbound state in which the eYFP/eCFP emission ratio is high and a sucrose-bound state in which eYFP/eCFP emission ratio which is low. **c.** Growth curves of PXO99^{A} (blue) and Δ*sux* (white) in NBN, NBN + 1 % sucrose or NBN + 1 % glucose (n=4). **d.** Growth curves of PXO99^{A} (blue) and Δ*sux* (white) in synthetic minimal medium (NSM) + 1 % sucrose (n=4). **e.** Sucrose uptake assay using the cytosolic genetically encoded FRET sensor FLIPsuc90μΔ1V (ref. (56)) in PXO99^{A} or Δ*suxC*. X-axis broken at time when sucrose was added to the microplate (grey dash); one cycle was 22 seconds. Decrease in emission intensity ratio corresponds to increase in cytosolic sucrose levels (n=4). All experiments repeated independently at least three times. See also S4 Fig.

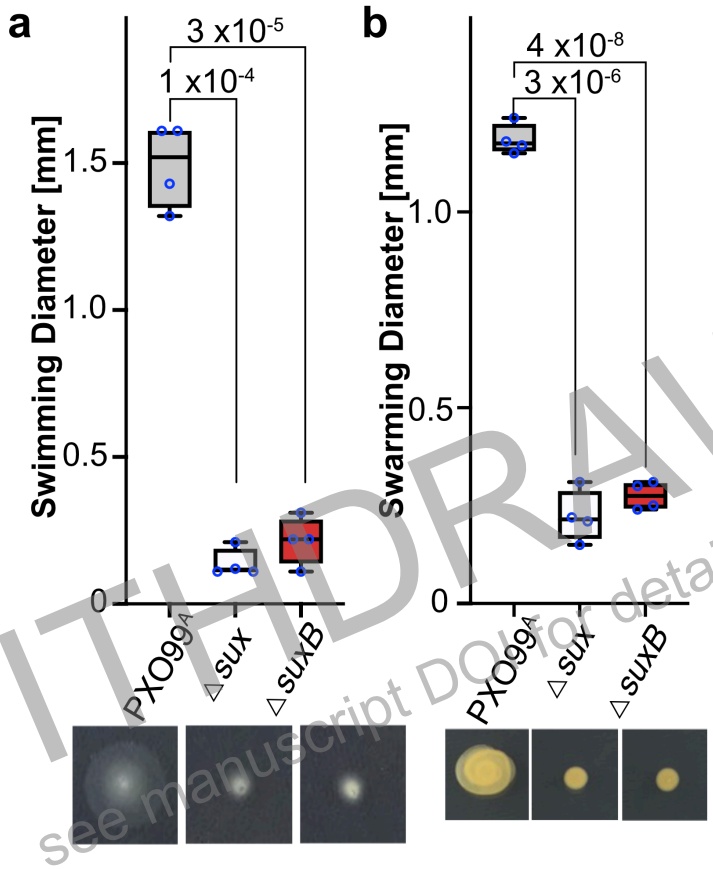

Figure 3. **Effects of mutations in *sux* genes on swimming and swarming motility. a.** *sux* mutants show reduced swimming motility in quantitative assays (n=4) and **b.** Swarming motility assays (n=4). Boxes extend from 25th to 75th percentiles and display median values as center lines. Whiskers plot minimum and maximum values and individual data points. Significance was calculated between two groups using unpaired two-tailed Student's *t* test at the 95 % confidence level and Welch's correction of unequal variances. Comparable results were obtained in three independent experiments. See also S5 and S6 Fig.

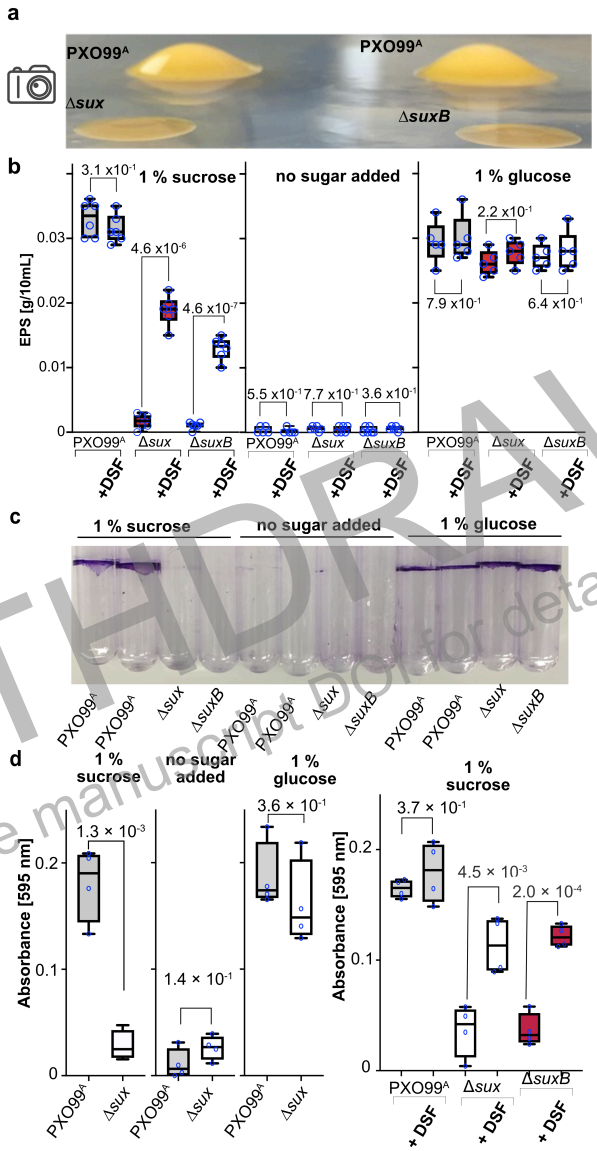

Figure 4. Effect of mutations in *sux* genes on EPS production and biofilm formation. a. Colony morphology on spot assays of *Xoo* grown uninverted on NBN + 1 % sucrose. Photography was performed horizontally (from the side, indicated by camera logo). **b.** Quantification of EPS produced by *Xoo* grown in liquid culture. The ability of wild-type and *sux* mutant strains to produce EPS was assessed (n≥4). The effect of DSF on EPS production in Δ*sux* and Δ*sux*B mutant strains of PXO99^A in the presence and absence of sucrose or glucose was measured. **c.** and **d.** Biofilm formation was determined in *Xoo* cultures in NBN + 1 % sucrose followed by crystal violet staining and quantified at OD_{595} (n≥4). Boxes extend from 25th to 75th percentiles and display median values as center lines. Whiskers plot minimum and maximum values and individual data points. Significance was calculated between two groups using unpaired two-tailed Student's *t*-Test at the 95 % confidence level and Welch's correction of unequal variances. Comparable results were obtained in three independent experiments. See also S7, S8, S9 and S10 Figures.

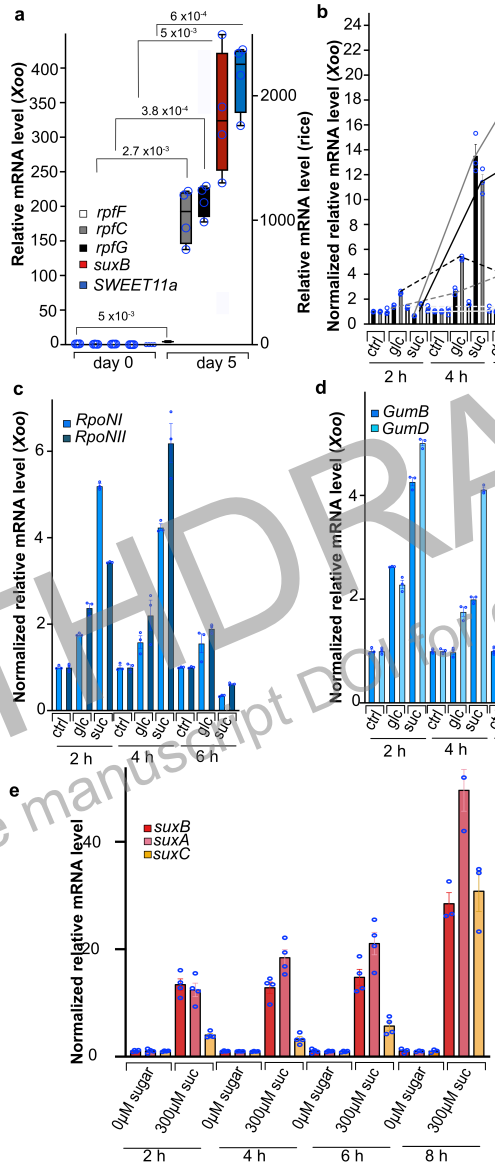

Figure 5. Regulation of quorum sensing genes during infection and *in vitro* by sugars. a. *in planta* qRT-PCR for *SWEET11a*, *suxB* and *rpfF*, *rpgG* and *rpfC* mRNA levels during PXO99^{A} infection. **b.** Effect of sugars on *rpfF*, *rpgG* and *rpfC* gene mRNA levels in PXO99^{A} grown in culture; **c.** Effect of sugars on mRNA levels of sigma factor RpoN genes. **d.** Effect of sugars on *gum* genes. e. Effect of sucrose on *sux* genes after 2h, 4h, 6h and 8h. Ctrl. No sugar added; glc: glucose; suc: sucrose. Data from three to four biological samples. Boxes extend from 25th to 75th percentiles and display median values as center lines. Whiskers plot minimum and maximum values and individual data points. Significance was calculated between two groups using unpaired two-tailed Student's *t* test at the 95 % confidence level and Welch's correction of unequal variances. Comparable results were obtained in three independent experiments. The $2^{-\Delta\Delta}$Ct method was used for relative quantification using 16S rRNA as reference. Transcript levels were then normalized to the control, and the control value was shown (at 1 PXO99A no sugar for *in vitro* and 0 day for *in planta*). See also S11 and S12 Figures.

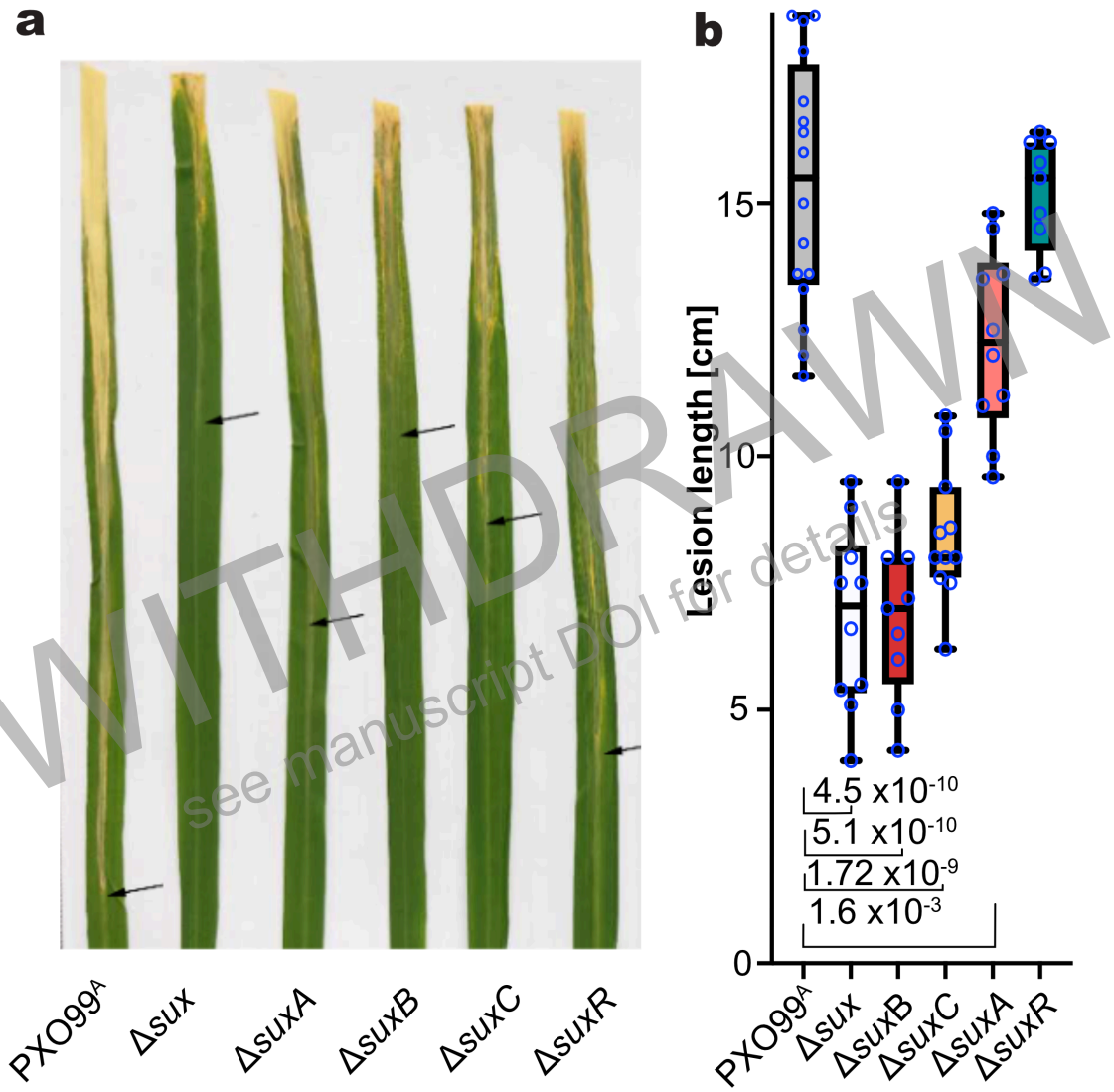

Figure 6. Role of *sux* genes for virulence of *Xoo* in rice. a. Leaf phenotypes in rice cultivar Nipponbare after clip-infection with PXO99^{A} and three *sux* mutants at 12 DPI in the rice cultivar Nipponbare. **b.** Quantification of lesion length (n=7). Boxes extend from 25th to 75th percentiles and display median values as center lines. Whiskers plot minimum and maximum values and individual data points. Significance was calculated between two groups using unpaired two-tailed Student's *t* test at the 95 % confidence level and Welch's correction of unequal variances. Similar results were obtained in three independent experiments. Significance listed only for pairs that showed a significant difference ($p < 0.05$). Data for complementation of mutants presented in S13 Figure.

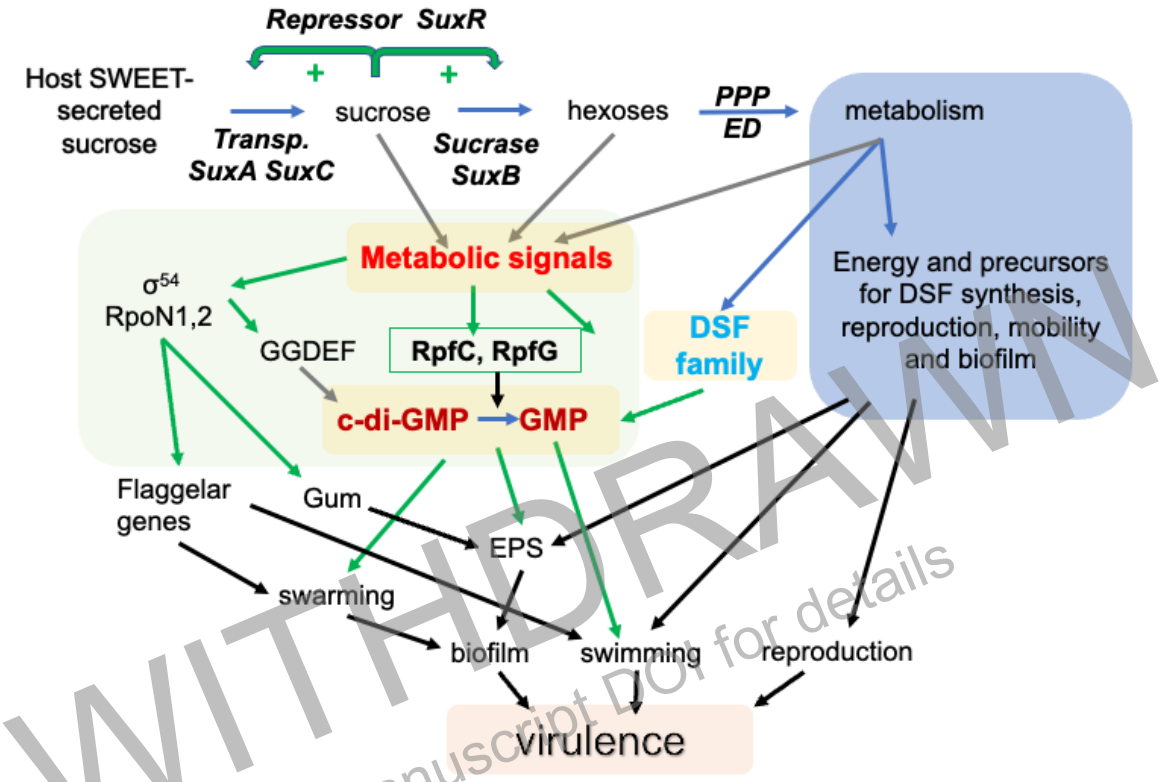

Figure 7. Model for dual roles of sucrose as carbon and energy source and signaling required for virulence of *Xoo*. *Xoo* induces SWEET-mediated sucrose efflux from the host. *Xoo* takes up sucrose via SuxA and SuxC transporters and metabolizes sucrose to hexoses via the suxB sucrase. These sugars are further metabolized via the Entner-Doudaroff (ED) and oxidative pentose phosphate pathway (PPP). The sugars or their downstream metabolites are then used for two major purposes: building blocks for cell division, biofilm production, synthesis of DSF family quorum sensing factors, as precursors for synthesis of other metabolites and to produce energy (ATP). Energy is required for biosynthetic processes as well as mobility (swimming and swarming) and thus ultimately for growth and many key aspects required for virulence (blue box). The *sux* genes are subject to SuxR-mediated feedforward regulation (bold green arrows and +) and induction during infection coincides with SWEET induction in the host; sucrose is sufficient for induction. Mutation of components of the sux sucrose utilization system lead reduced swimming, swarming, EPS/biofilm production, reproduction and virulence as shown in this manuscript. On top of the metabolic roles of sucrose and its metabolic products, these also serve in signaling processes (green box). We show here that transcripts for the two components histidine kinase relay system with a dual role in di-guanine cyclase activity (82) RpfC and RpfG are also sucrose-inducible, possibly sensitizing the cells to the quorum sensing family during infection. It is well established that quorum sensing factors trigger biofilm production, motility and swarming and are key to virulence (83). At the same time, sucrose or its metabolites induce the genes for the sigma-54 factors RpoN1 and RpoN2 as shown here. The sigma factors are essential for virulence as well, and mutant analyses show that in the absence of the sigma factors, flagellar assembly

is blocked, preventing effective swimming and swarming, *gum* gene transcripts responsible for EPS are produced at reduced rates and mRNAs for GGDEF genes with unknown function, but homology to guanylate cyclases, are produced to lower levels (60). The regulatory network presented here contains many unknowns, e.g., what is the actual inducer of gene expression, what are the receptors, and the network is highly complex with differential roles of the two sigma factors and the different DSF family forms. Taken together, *Xoo* makes use of the host secreted sucrose and virulence likely depends on both signaling and metabolic roles of sucrose or its downstream metabolites. Blue arrows: metabolic conversions; thin green arrows: transcriptional regulation; grey arrows predicted links; Black arrows: effects.

Supporting information

S1 Table. Homologs of the *sux* gene cluster in *Xoo* and *Xcc*

[a] in reference to *Xcc* homologs from Blanvillain and Meyer (33)

[b] The upper line for the nucleotide identity and the lower for the amino acid identity between *Xoo* and *Xcc* genes and proteins, respectively.

S2 Table. Conservation of the *sux* locus among *Xanthomonas* spp.

S3 Table. Bacterial strains and plasmids used in this study.

S4 Table. Oligonucleotides used in this paper.

S5 Table. Absolute Ct values for qRT-PCR experiments

S6 Table. OD_{600} and CFU/mL of PXO99^{A} and Δ*sux* mutant

S1 Figure. Potential functions of *Xoo*-encoded *sux* gene products in sucrose uptake and utilization in the rice leaf xylem. Model of the feeding hypothesis in which the *sux* gene cluster components enable *Xoo* to utilize sucrose exported by SWEETs from the xylem parenchyma into the apoplasmic space. The activity of the SWEETs is triggered by TAL effectors from *Xoo*. Sucrose is imported across the outer membrane of *Xoo* by SuxA, a TonB-dependent receptor, then taken up across the inner membrane with the help of SuxC, a major facilitator superfamily (MFS) sucrose transporter. Intracellular sucrose is detected by SuxR, a LacI-type repressor, which derepresses the other *sux* genes in a sucrose-dependent manner. SuxB hydrolyzes sucrose to produce glucose and fructose, which are further metabolized in the cell. TonB is typically involved in transducing energy to multiple TBDRs, and is encoded by a separate gene.

S2 Figure. Conservation of *sux* gene cluster in different *Xanthomonas* spp. Phylogenetic tree was generated using an alignment of a concatenated *sux* ORF cluster sequence (only coding regions were used as a concatenated sequence). Sequences from 14 species were used: *X. arboricola* pv. *juglandis*, *X. citri* pv. *malvacearum*, *X. vasicola* pv. *vasculorum*, *X. cucurbitae*, *X. phaseoli*, *X. oryzae* pv. *oryzicola*, *X. oryzae* pv. *oryzae*, *X. hortorum*, *X. fragariae*, *X. campestris* pv. *vesicatoria*, *X. vesicatoria*, *X. campestris* pv. *campestris*, *X. translucens* pv. *translucens*, and *X. albilineans.*

S3 Figure: **Sucrose-dependent derepression of *sux* genes by SuxR. a.** **a.** Predicted binding region for the LacI-type HDH domain transcriptional regulator SuxR found by homology to the predicted binding site of *Xam* and *Xag* homologs from the RegPrecise database (54). **b.** 3D homology model of SuxR (Magenta) based on the structure of the LacI transcriptional regulator CelR in complex with cellobiose (PDB ID: 5ysz). **c.** *suxA* transcript levels during infection of Kitaake as determined using qRT-PCR (0, 3, 5, 7 and 10 days after infection). **d.** qRT-PCR analyses of *suxB* and *suxC* mRNA levels in *Xoo* growing on NB without sugar or

1 % sucrose or glucose in Δ*suxR*. Values are derived from four biological replicates, each with three technical replicates. Boxes extend from 25th to 75th percentiles and display median values as center lines. Whiskers plot minimum and maximum values and individual data points. Significance was calculated between two groups using unpaired two-tailed Student's *T* test at the 95 % confidence level and Welch's correction of unequal variances. The $2^{-\Delta\Delta}$Ct method was used for relative quantification with 16S rRNA as reference. Relative mRNA levels *in vitro* are normalized to 1 for values for data from PXO99^{A} without added sugar. Relative mRNA levels *in planta* are normalized to 1 for values for data at 0 day. Comparable results were obtained in three independent experiments. DBD: DNA binding domain; N-RD: N-terminus regulatory domain; C-RD: C-terminus regulatory domain.

S4 Figure. Growth and colony phenotypes of *sux* mutants. Growth and colony phenotypes of *sux* mutants. a. Mucoid and dry colony phenotypes of sux mutants on NB plates with addition of low concentration of sugar (1.5, 3, 6, 12 and 30 µM) and **b.** on NBN, NBN + 1 % sucrose or NBN + 1 % glucose **c.** Growth curves of PXO99^{A} (blue) and Δ*sux* (white) in synthetic minimal medium (NSM) or NSM + 1 % glucose (n=4). *E*xperiments were conducted at least three times independently. Genotypes are numbered: 1 wild type control, PXO99; 2 Δ*sux*; 3 Δ*suxA*; 4 Δ*suxB*; 5 Δ*suxC*; 6 Δ*suxR*; complementation with constructs using the *E. coli* Lac promoter: 7 Δ*suxA*/*suxA*; 9 Δ*suxB*/*suxB*; 11 Δ*suxC*/*suxC*; 13 Δ*suxR*/*suxR*; and complementation with constructs using native *Xoo* promoters; 8 Δ*suxA*/pA-*suxA*; 10 Δ*suxB*/pA-*suxB*; 12 Δ*suxC*/pC-*suxC*; 14 Δ*suxR*/pR-*suxR.*

S5 Figure. Swimming and swarming motility of Δ*sux* mutant. a. Swimming on solid NBN + 1 % sucrose and 0.3 % agar. **b.** Swarming assays on solid NBN + 1 % sucrose and 0.6 % agar. Comparable results were obtained in three independent experiments.

S6 Figure. EPS, swimming and swarming motility of Δ*suxR* mutant. a. Swimming and swarming on solid NBN + 1 % sucrose and 0.3 % agar or 0.6 % agar, respectively. **b.** Similar assays on round petri dishes for swarming mobility and **c.** for swimming motility. Comparable results were obtained in three independent experiments.

S7 Figure. Δ*sux* and Δ*suxB* mutants show complete EPS deficiency a. Colony phenotype of PXO99^{A} and Δ*sux* mutant and **b.** Δ*suxR* mutant on solid NBN + 1 % of sucrose grown uninverted for day 2, day 3 and day 4. Photography was performed vertically (from the top). **c.** Colony morphology on inverted plates (NBN + 1 % of sucrose). Photography was performed horizontally (from the side). Comparable results were obtained in three independent experiments.

S8 Figure. EPS production in the presence of sucrose or glucose. Quantification of EPS. The ability of wild-type PXO99^{A} and *sux* mutant strains to produce EPS was assessed in the presence of sucrose or glucose. Data from three

biological samples. Boxes extend from 25th to 75th percentiles and display median values as center lines. Whiskers plot minimum and maximum values and individual data points. Significance was calculated between two groups using unpaired two-tailed Student's t-Test at the 95 % confidence level and Welch's correction of unequal variances. Comparable results were obtained in three independent experiments.

S9 Figure. Sucrose uptake-dependent EPS production in complemented strains. Quantification of EPS production in the wild type strain PXO99^{A}, in the Δ*suxB* mutant and in a Δ*suxB* mutant complemented with the *suxB* gene driven from the lacZ promoter in the presence and absence of sucrose (n=3). Comparable results were obtained for the sucrose induction in three independent experiments.

S10. Figure. Sucrose uptake and biofilm formation. a. Biofilm formation assays of the wild type strain PXO99^{A} and the *Δsux* and *ΔsuxB* mutants in a 96-well plate. **b.** Qualitative and quantitative assays for biofilm formation assays in glass tube when complemented with DSF. Biofilm formation was determined in *Xoo* cultures in NB + 1 % sucrose followed by crystal violet staining. Comparable results were obtained for the sucrose induction in three independent experiments.

S11 Figure. Growth of *Xoo* on sugar. Growth of PXO99^{A} in the presence or absence of 300μM sucrose or glucose. Similar results were obtained in three independent experiments.

S12 Figure. Regulation of genes in Δ*suxR* mutant. Gene expression on mRNA levels in PXO99^{A} and Δ*suxR* mutant. The 2-ΔΔCt method was used for quantification. The $2^{-\Delta\Delta}$Ct method was used for relative quantification with 16S rRNA as reference. Transcript levels were then normalized to the control, and the control value was shown (at 1 PXO99^{A} no sugar).

S13 Figure. Virulence of complemented strains using synthetic and endogenous promoters of *sux* genes. a. Leaf phenotypes in rice cultivar Nipponbare after clip infection with PXO99^{A}, *sux* mutants and complementation strains at 12 DPI. **b.** Quantification of lesion length for two types of complementation strains: complementation with constructs using *E. coli* Lac promoter in Δ*suxA*/*suxA*; Δ*suxB*/*suxB*; Δ*suxC*/*suxC*; and Δ*suxR*/*suxR*; and complementation with constructs using native *Xoo* promoters in Δ*suxA*/pA-*suxA*; Δ*suxB*/pA-*suxB*; Δ*suxC*/pC-*suxC*; and Δ*suxR*/pR-*suxR*. Boxes extend from 25th to 75th percentiles and display median values as center lines. Whiskers plot minimum and maximum values and individual data points. Significance was calculated between two groups using unpaired two-tailed Student's t-Test at the 95 % confidence level and Welch's correction of unequal variances. Similar results were obtained in three independent experiments. Significance listed only for pairs that showed a significant difference ($p < 0.05$).